

INVESTIGATION OF THE EFFECTS OF DIFFERENT MACROSTRUCTURES  
ON CONJUGATED POLYMER BASED AMPEROMETRIC BIOSENSOR  
PERFORMANCE

A THESIS SUBMITTED TO  
THE GRADUATE SCHOOL OF NATURAL AND APPLIED SCIENCES  
OF  
MIDDLE EAST TECHNICAL UNIVERSITY

BY

ECE BÜBER

IN PARTIAL FULFILLMENT OF THE REQUIREMENTS  
FOR  
THE DEGREE OF MASTER OF SCIENCE  
IN  
CHEMISTRY

JULY 2018



Approval of the thesis:

**INVESTIGATION OF THE EFFECTS OF DIFFERENT  
MACROSTRUCTURES ON CONJUGATED POLYMER BASED  
AMPEROMETRIC BIOSENSOR PERFORMANCE**

submitted by **ECE BÜBER** in partial fulfillment of the requirements for the degree of  
**Master of Science in Chemistry Department, Middle East Technical University**  
by,

Prof. Dr. Halil Kalıpçılar  
Dean, Graduate School of **Natural and Applied Sciences** \_\_\_\_\_

Prof. Dr. Cihangir Tanyeli  
Head of Department, **Chemistry** \_\_\_\_\_

Prof. Dr. Levent Toppare  
Supervisor, **Chemistry Dept., METU** \_\_\_\_\_

**Examining Committee Members:**

Prof. Dr. Ali Çırpan  
Chemistry Dept., METU \_\_\_\_\_

Prof. Dr. Levent Toppare  
Chemistry Dept., METU \_\_\_\_\_

Prof. Dr. Yasemin Arslan Udum  
Technical Sciences Vocational School, Gazi University \_\_\_\_\_

Assoc. Prof. Dr. Emren Nalbant Esentürk  
Chemistry Dept., METU \_\_\_\_\_

Assoc. Prof. Dr. İrem Erel Göktepe  
Chemistry Dept., METU \_\_\_\_\_

**Date:** \_\_\_\_\_ 16.07.2018 \_\_\_\_\_

**I hereby declare that all information in this document has been obtained and presented in accordance with academic rules and ethical conduct. I also declare that, as required by these rules and conduct, I have fully cited and referenced all material and results that are not original to this work.**

Name, Last name : Ece BÜBER

Signature :

## **ABSTRACT**

### **INVESTIGATION OF THE EFFECTS OF DIFFERENT MACROSTRUCTURES ON CONJUGATED POLYMER BASED AMPEROMETRIC BIOSENSOR PERFORMANCE**

Büber, Ece  
MSc, Department of Chemistry  
Supervisor : Prof. Dr. Levent Toppare

July 2018, 72 pages

In this thesis, the use of different macrostructures in the surface design of conjugated polymer based amperometric biosensors was investigated since surface properties play a crucial role in the performance of biosensors. Conjugated polymers (CPs) provide biosensors superior features since they exhibit conductivity, high mechanical strength and processability. Moreover, phthalocyanines (Pcs) are promising molecules for biosensor applications due to their electronic properties, rich redox chemistry and high electrochemical stability. In addition to phthalocyanines, dendrimers are suitable host molecules for accommodation of guest molecules due to their three-dimensional structure having an internal void space. Especially, poly(amidoamine) (PAMAM), can be used in biosensor applications since it contains a number of terminal amino groups which enhances the attachment of biomolecules. Multi-walled carbon nanotubes (MWCNTs) have also extensively used in biosensor applications since they are compatible with biomolecules in addition to their mechanical strength, stability and conductivity properties. By taking the advantages of these materials, two novel glucose biosensors; CPs/MWCNTs/ZnPc and CPs/MWCNTs/PAMAM were fabricated. Their operational and kinetic parameters and surface features were characterized and the biosensors were successfully tested for real time analyses.

Keywords: Electrochemical biosensors, phthalocyanines, dendrimers, carbon nanotubes, glucose oxidase

## ÖZ

### FARKLI MAKRO YAPILARIN KONJUGE POLİMER BAZLI AMPEROMETRİK BİYOSENSÖR PERFORMANSI ÜZERİNE ETKİLERİNİN ARAŞTIRILMASI

Büber, Ece  
Yüksek Lisans, Kimya  
Tez Yöneticisi : Prof. Dr. Levent Toppare

Temmuz 2018, 72 sayfa

Biyosensörlerin yüzey özellikleri performansları üzerinde çok önemli bir rol oynar. Bu nedenle, bu tezde, konjuge polimer esaslı amperometrik biyosensörlerin yüzey tasarımında farklı makroyapıların kullanımı araştırılmıştır. İletken polimerler (CPs) iletkenlik, yüksek mekanik dayanıklılık ve işlenebilirlik özelliklerinden dolayı biyosensörlere üstün nitelikler sağlarlar. Ayrıca, ftalosiyanimler (Pcs) de zengin redoks kimyası ve elektrokimyasal kararlılık gibi elektronik özelliklerinden dolayı biyosensör uygulamaları için uygun moleküllerdir. Ek olarak, dendrimerler üç boyutlu yapılarındaki dahili boşluk oranından dolayı konuk moleküllerin yerleşmesi için uygun konak moleküllerdir. Özellikle, poli(amidoamin) (PAMAM) yapısı biyomoleküllerin bağlanmasını güçlendiren terminal amino grupları içermesi sebebiyle biyosensör uygulamalarında etkili bir malzemedir. Ayrıca, çok duvarlı karbon nanotüpler (MWCNTs) mekanik mukavemet, stabilite ve yüksek iletkenlik özelliklerine ek olarak biyoyumluluk gösterdikleri için biyosensör uygulamalarında yaygın olarak kullanılmaktadır. Bütün bu yapıların avantajlarından yararlanarak, CPs/MWCNTs/ZnPc ve CPs/MWCNTs/PAMAM kombinasyonlarında iki yeni glikoz biyosensörü oluşturulmuş, operasyonel ve kinetik parametreleri ile yüzey özellikleri karakterize edilmiş ve biyosensörler gerçek zamanlı analizler için başarılı bir şekilde test edilmiştir.

Anahtar Kelimeler: Elektrokimyasal biyosensör, konjüge polimer, ftalosiyenin, dendrimer, karbon nanotüp, glikoz oksidaz

To my precious mom and granny...



## ACKNOWLEDGMENTS

First of all, I would like to express my greatest appreciation to my supervisor Prof. Dr. Levent Toppare for his faith in me. There is no word to express my gratitude for his support, guidance, encouragement and valuable advices. Knowing that he will always be there for me whenever I need is a feeling beyond words.

I would also like to acknowledge Prof. Dr. Ali Çırpan, Prof. Dr. Yasemin Udum Arslan, Assoc. Prof. Dr. Emren Nalbant Esentürk and Assoc. Prof. Dr. İrem Erel Göktepe as the second reader of this thesis, and I am gratefully thankful to their valuable comments.

I wish to thank my mentors Dr. Melis Kesik and Dr. Saniye Söylemez for everything that I have learnt about biosensors. Without their passionate participation and experience, this thesis study could not have been completed successfully. I appreciate for their encouragement, motivation, support, and endless help.

I would like to thank Assoc. Prof. Dr. Mine İnce and her research group for the synthesis of zinc phthalocyanine molecule since with utilization of this structure, my thesis study became better in quality.

I owe great thanks to Seza Göker, Gönül Hızalan, Tuğba Ceren Gökoğlan, Hande Özel, Ecem Aydan, Janset Turan and Ebru Işık for their great support and providing an excellent working environment during my research period. They make these years unforgettable.

I am faithfully thankful to Begüm Avcı and Merve Nur Güven for their real friendship, support and motivation since the beginning of our journey in this department. I know that they are always with me.

I cannot forget my dearest friends who cheered me on, went through hard times together, and celebrated each accomplishment: Aysel Akgemci, Negin Razizadeh,

Nami Çağan Yüksel, Erdem Canbalaban, Furkan Doğramacı, Baturay Özel, Berkay Baykara, Cenk Tüysüz and Hakan Mert.

I express my deepest sense of gratitude to Sevil Çalışkan for being a friend beyond words. It is not easy to live with someone who you don't know at all, but we turned it into a real friendship. Our story began at a dormitory room and I know it will last till the end.

I am deeply grateful to Elifcan Özyıldırım for being a sister to me. Although we have always been in different cities, even in different countries, she has always been there for me. Since 2008, she believes in me and makes my life better.

Special and sincerest thanks must go to Eda Bolayır, not only a friend but also a teammate. We have achieved everything together, hand in hand. The trips, tea-times, girl's night outs, breakfasts, movie nights, shopping times, debates, lab memories and nonsense conversations are all the special things that make us the "Bolber Team". She is an amazing tiny little human being. Thanks for her enthusiasm, pride and curiosity to share my map of the world.

I would like to share my faithful gratitude with Erencan Duymaz for his amazing love, extraordinary thoughtfulness, understanding, trust and encouragement. I could not be able to survive throughout this year without his love and endless support. He suddenly came into my life and became the most beautiful thing. He makes everything brighter. I am thankful for every moment that I live with him.

Thank you my family: my granny, grandpa, aunts, uncles and cousins. You have always been there for me from the time I was a baby. You should know that your support and encouragement was worth more than I can express on a paper. Thank you for providing me an extremely amazing family environment.

Finally, there is no word to express my love and gratitude to my dear mom. She is my idol, my best friend, my life, and the best gift for me. I am the luckiest person in the world being the daughter of such a strong woman. Today, I am what I am thanks to her. Without her, I would not be able to achieve anything throughout my life.

## TABLE OF CONTENTS

ABSTRACT .....	v
ÖZ .....	vii
ACKNOWLEDGMENTS .....	xi
TABLE OF CONTENTS .....	xiii
LIST OF TABLES .....	xvi
LIST OF FIGURES .....	xvii
CHAPTERS	
1. INTRODUCTION .....	1
1.1. Biosensors .....	1
1.1.1. Types of Biosensors .....	3
1.1.1.1. Electrochemical Biosensors .....	4
1.1.2. Immobilization Techniques.....	8
1.1.2.1. Physical Adsorption .....	9
1.1.2.2. Covalent Binding .....	9
1.1.2.3. Entrapment .....	10
1.1.2.4. Cross linking .....	11
1.1.3. Glucose Biosensors .....	12
1.1.3.1. Glucose oxidase enzyme (GOx).....	13
1.2. Conjugated Polymers (CPs) .....	14
1.2.1. Theory of Conjugated Polymers .....	14
1.2.2. Conjugated Polymers in Biosensor Applications.....	16
1.3. Carbon Nanotubes (CNTs).....	17
1.3.1. Carbon Nanotubes in Biosensor Applications .....	18
1.4. Macrostructures in Biosensor Design .....	19
1.4.1. Phthalocyanines (Pcs) .....	20
1.4.1.1. Metal Phthalocyanines (MPcs) .....	21
1.4.2. Dendrimers .....	23
1.4.2.1. Poly(amidoamine) (PAMAM) .....	25

1.5. Aim of This Thesis.....	26
2. PFLA/ZnPc/MWCNTs/GOx BIOSENSOR .....	29
2.1. Experimental.....	29
2.1.1. Materials and Methods.....	29
2.1.2. Preparation of the Biosensor .....	30
2.1.3. Amperometric Measurements .....	31
2.1.4. Optimization of Biosensor Performance.....	31
2.1.5. Characterizations.....	32
2.1.5.1. Analytical and Kinetic Characterizations .....	32
2.1.5.2. Surface Characterizations .....	33
2.1.6. Sample Application.....	34
2.2. Results and Discussion .....	34
2.2.1. Optimization Studies.....	34
2.2.1.1. Optimization of the Biosensor Parameters .....	34
2.2.1.2. Determination of the Best Combination .....	39
2.2.2. Characterizations.....	40
2.2.2.1. Analytical and Kinetic Characterizations .....	40
2.2.2.2. Surface Characterizations .....	44
2.2.3. Application of the Biosensor .....	46
3. PFLA/PAMAM/MWCNTs/GOx BIOSENSOR .....	47
3.1. Experimental.....	47
3.1.1. Materials and Methods.....	47
3.1.2. Preparation of the Biosensor .....	48
3.1.3. Amperometric Measurements .....	49
3.1.4. Optimization of Biosensor Performance.....	49
3.1.5. Characterizations.....	49
3.1.5.1. Analytical and Kinetic Characterizations .....	49
3.1.5.2. Surface Characterizations .....	50
3.1.6. Sample Application.....	50
3.2. Results and Discussion .....	50
3.2.1. Optimization Studies.....	50
3.2.1.1. Optimization of the Biosensor Parameters .....	50

3.2.1.2. Determination of the Best Combination .....	54
3.2.2. Characterizations.....	55
3.2.2.1. Surface Characterizations.....	55
3.2.2.2 Analytical and Kinetic Characterizations.....	57
3.2.3. Application of the Biosensor.....	60
4. CONCLUSION .....	63
REFERENCES.....	65

## LIST OF TABLES

### TABLES

<b>Table 2.1.</b> Comparison of glucose biosensors in the literature. ....	43
<b>Table 2.2.</b> Results of glucose analysis in beverages. ....	46
<b>Table 3.1.</b> Comparison of glucose biosensors in the literature. ....	60
<b>Table 3.2.</b> Results of glucose analysis in beverages. ....	61

## LIST OF FIGURES

### FIGURES

<b>Figure 1.1.</b> Schematic representation of a biosensor.....	2
<b>Figure 1.2.</b> Biosensors according to the types of biomolecules and transducers .....	3
<b>Figure 1.3.</b> Working principles of different generations of biosensors.....	5
<b>Figure 1.4.</b> A typical three electrode electrochemical cell configuration .....	7
<b>Figure 1.5.</b> Enzyme immobilization techniques.....	8
<b>Figure 1.6.</b> Glucose oxidase reaction mechanism .....	13
<b>Figure 1.7.</b> Band structures of insulator materials, semiconductors and metals .....	15
<b>Figure 1.8.</b> Carbon nanotubes: single-walled carbon nanotubes (SWCNTs) on the left; and multi-walled carbon nanotubes (MWCNTs) on the right.....	18
<b>Figure 1.9.</b> General structure of phthalocyanines .....	20
<b>Figure 1.10.</b> General structure of metal phthalocyanines.....	22
<b>Figure 1.11.</b> Anatomy of a dendrimer .....	24
<b>Figure 1.12.</b> Structure of PAMAM dendrimers .....	26
<b>Figure 2.1.</b> Schematic representation of PFLA/MWCNTs/ZnPc/GOx Biosensor ...	30
<b>Figure 2.2.</b> Amperometric measurement procedure.....	31
<b>Figure 2.3.</b> The effect of polymer amount on biosensor response (in 50.0 mM PBS, pH 7.0, 25°C). Error bars show the standard deviation (SD) of three measurements. ....	35
<b>Figure 2.4.</b> The effect of MWCNTs amount on biosensor response (in 50.0 mM PBS, pH 7.0, 25°C). Error bars show the standard deviation (SD) of three measurements.....	36
<b>Figure 2.5.</b> The effect of ZnPc amount on biosensor response (in 50.0 mM PBS, pH 7.0, 25°C). Error bars show the standard deviation (SD) of three measurements. ....	37
<b>Figure 2.6.</b> The effect of loaded enzyme amount on biosensor response (in 50.0 mM PBS, pH 7.0, 25°C). Error bars show the standard deviation (SD) of three measurements.....	38
<b>Figure 2.7.</b> The effect of pH on biosensor response (in 50 mM sodium acetate buffer at pH 4.0; 5.0; 5.5, 50 mM PBS at pH 6.0; 6.5;7.0;7.5 and 50 mM Tris buffer at pH	

8.0 and 9.0, 25°C). Error bars show the standard deviation (SD) of three measurements.....	39
<b>Figure 2.8.</b> The effect of different surface modifications on performance of glucose biosensors (in 50.0 mM PBS, pH 7.0, 25°C). Error bars show the standard deviation (SD) of three measurements.....	40
<b>Figure 2.9.</b> Calibration curve for glucose (in 50 mM PBS, pH 7.0, 25°C). Error bars show standard deviation (SD) of three measurements.....	41
<b>Figure 2.10.</b> Biosensor responses to glucose and interfering substances (in 50 mM PBS, pH 7.0, 25 °C).....	42
<b>Figure 2.11.</b> Cyclic voltammograms resulting from pristine PFLA, PFLA/MWCNT, PFLA/MWCNT/ZnPc and PFLA/MWCNT/ZnPc/GOx in 5.0 mM Fe(CN) <sub>6</sub> <sup>3-/4-</sup> containing 0.1 M KCl. ....	45
<b>Figure 2.12.</b> SEM images of (A) pristine PFLA; (B) PFLA/MWCNT/ZnPc; (C) PFLA/MWCNT/ZnPc/GOx under optimized conditions. ....	46
<b>Figure 3.1.</b> Schematic representation of PFLA/MWCNTs/PAMAM/GOx Biosensor .....	48
<b>Figure 3.2.</b> The effect of polymer amount on biosensor response (in 50.0 mM PBS, pH 7.0, 25°C). Error bars show the standard deviation (SD) of three measurements. ....	51
<b>Figure 3.3.</b> The effect of MWCNTs amount on biosensor response (in 50.0 mM PBS, pH 7.0, 25°C). Error bars show the standard deviation (SD) of three measurements.....	52
<b>Figure 3.4.</b> The effect of PAMAM concentration on biosensor response (in 50.0 mM PBS, pH 7.0, 25°C). Error bars show the standard deviation (SD) of three measurements.....	53
<b>Figure 3.5.</b> Effect of enzyme amount on biosensor response (in 50.0 mM PBS, pH 7.0, 25°C). Error bars show the standard deviation (SD) of three measurements. ....	53
<b>Figure 3.6.</b> Effect of pH (in 50 mM sodium acetate buffer at pH 4.0; 5.0; 5.5, 50 mM PBS at pH 6.0; 6.5; 7.0; 7.5 and 50 mM tris buffer at pH 8.0 and 9.0) on biosensor response. Error bars show the standard deviation (SD) of three measurements.....	54

<b>Figure 3.7.</b> Structures of PAMAM G2 and PAMAM G4.....	55
<b>Figure 3.8.</b> Cyclic voltammograms resulting from a bare graphite, PFLA/MWCNT, PFLA/MWCNT/PAMAM and PFLA/MWCNT/PAMAM/GOx in 5.0 mM Fe(CN) <sub>6</sub> <sup>3-/4-</sup> containing 0.1 M KCl. ....	56
<b>Figure 3.9.</b> SEM images of (A) pristine PFLA; (B) PFLA/MWCNT; (C) PFLA/MWCNT/PAMAM (D) PFLA/MWCNT/PAMAM/GOx under the optimized conditions. ....	57
<b>Figure 3.10.</b> Calibration curve for glucose (in 50 mM PBS, pH 7.0, 25 °C). Error bars show standard deviation of three measurements. ....	58
<b>Figure 3.11.</b> Biosensor responses to glucose and interfering substances (in 50 mM PBS, pH 7.0, 25 °C). ....	59

## LIST OF ABBREVIATIONS

<b>Ag</b>	Silver
<b>CB</b>	Conduction Band
<b>CE</b>	Counter Electrode
<b>CNTs</b>	Carbon Nanotubes
<b>CP</b>	Conjugated Polymer
<b>CV</b>	Cyclic Voltammetry
<b>DMF</b>	Dimethylformamide
<b>E<sub>g</sub></b>	Band gap
<b>FAD</b>	Flavin Adenine Dinucleotide
<b>GA</b>	Glutaraldehyde
<b>GOx</b>	Glucose Oxidase
<b>HOMO</b>	Highest Occupied Molecular Orbital
<b>LOD</b>	Limit of Detection
<b>LUMO</b>	Lowest Unoccupied Molecular Orbital
<b>MPc</b>	Metal Phthalocyanine
<b>MWCNTs</b>	Multi-walled Carbon Nanotubes
<b>NADH</b>	Nicotinamide adenine dinucleotide
<b>PAMAM</b>	Poly(amidoamine)
<b>PBS</b>	Phosphate-buffered Saline
<b>Pc</b>	Phthalocyanine
<b>PFLA</b>	poly[9,9-di-(2-ethylhexyl)-fluorenyl-2,7-diyl] end capped with N,N-bis(4- methylphenyl)-4-aniline
<b>Pt</b>	Platinum
<b>RE</b>	Reference Electrode
<b>RSD</b>	Relative Standard Deviation

<b>SEM</b>	Scanning Electron Microscope
<b>SD</b>	Standard Deviation
<b>VB</b>	Valence Band
<b>WE</b>	Working Electrode
<b>ZnPc</b>	Zinc Phthalocyanine



## CHAPTER 1

### INTRODUCTION

#### 1.1. Biosensors

For biosensors, two commonly cited definitions by S.P.J. Higson [1] and D.M. Frazer [2] are; “a biosensor is a chemical sensing device in which a biologically derived recognition entity is coupled to a transducer, to allow the quantitative development of some complex biochemical parameter,” and “a biosensor is an analytical device incorporating a deliberate and intimate combination of a specific biological element (that creates a recognition event) and a physical element (that transduces the recognition event).” Briefly, a biosensor is a sensing device containing a biological recognition element that is integrated within or connected to a transducer which converts the biochemical signal into an easily measurable format [3].

In 1962, Leland C. Clark developed the first glucose enzyme electrode based on the entrapped enzyme to an oxygen electrode with a semipermeable dialysis membrane. The entire field of biosensors can be originated from this enzyme electrode. Clark’s original patent [4] includes the utilization of enzymes for the conversion of electro-inactive reactants into electroactive products. Since then, researchers from various fields of science have gathered together to build more accurate, mature and reliable biosensing devices.

Although there are a number of different tests and methods to detect different biomarkers, which can be used in the diagnosis of various health conditions, these methods have time constraints and require trained staff, costly equipment and hospital attendance. Therefore, much practical methods can provide cost effective diagnosis without requiring any specific place or condition [5]. For this purpose, biosensor technology has been developing as a multidisciplinary and expanding field since biosensors are simple to operate, selective and rapid systems and offer ease of

fabrication with minimal sample pretreatment [6]. In today's technological world, biosensors have applications in clinical analysis, environmental monitoring, food industry, genetic engineering and bioprocess monitoring [7].

Most of the biosensors consist of two main components; a biomolecule and a transducer. The biomolecule selectively recognizes the analyte that is being monitored. This part can be enzymes, tissues, antibodies, receptors or nucleic acids. The transducer converts the biological signal into a detectable format. The transducing can be in a form of generation of an electroactive species, a change in conductivity or a change in optical properties [5]. Figure 1.1 shows the general schematic representation of a biosensor.

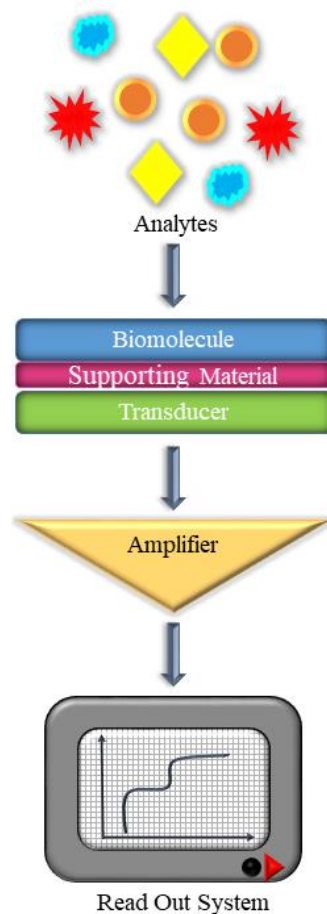


**Figure 1.1.** Schematic representation of a biosensor

### 1.1.1. Types of Biosensors

Specific interactions between the biomolecule and the analyte cause changes in physical and chemical properties which can be detected by the transducer. Biosensors can be categorized according to the types of biomolecules and transducers as given in Figure 1.2.

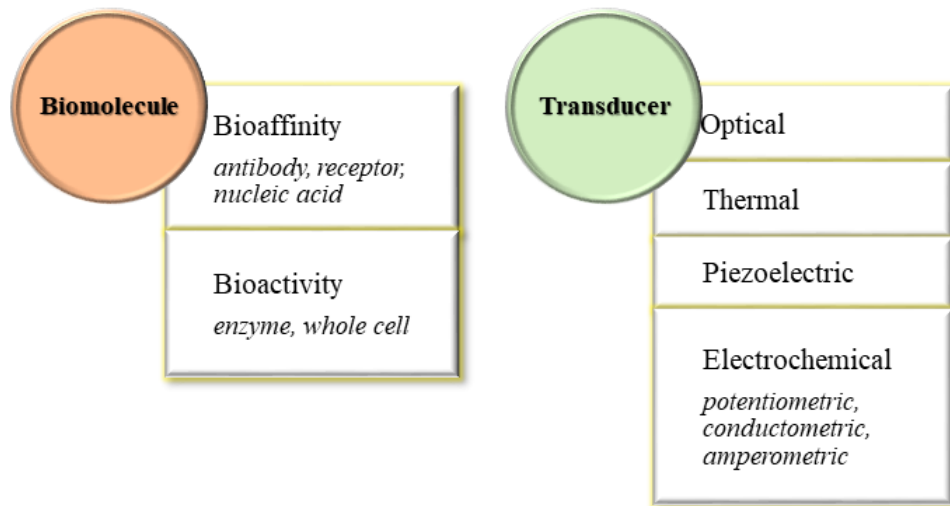


**Figure 1.2.** Biosensors according to the types of biomolecules and transducers

Optical biosensors operate on the principle of measurement of the output transduced light signal as a result of a biochemical reaction. These devices include a material on a cable that can produce an optical signal related to the analyte concentration in the sample. Optical biosensor can be utilized for the measurement of electrochemiluminescence or optical diffraction [8].

Thermal biosensors make use of temperature changes in the reaction medium as a result of absorption or generation of heat, which is one of the fundamental characteristics of biological reactions. These biosensors combine the immobilized biomolecules with temperature sensors. As a result of the interaction of the analyte with the biomolecule, the total absorbed or produced heat, which is proportional to the

total number of molecules and the molar enthalpy, is monitored according to the concentration of the analyte [9].

Piezoelectric biosensors are sensitive mass to-frequency transducers. In other words, they sense the changes in the density, viscosity or mass of analytes in contact with the active surface. These devices detect the analyte on the basis of generation of electric dipoles on subject to an anisotropic natural crystal to mechanical stress [10].

All of these types of biosensors have certain drawbacks. Although optical biosensors are very sensitive, they cannot be used in turbid media. Thermal biosensor cannot give results in the case of very little heat change and they are not easy to handle. Therefore, electrochemical biosensors have appeared as the mostly preferred biosensor type since they have the potential to overcome most of the drawbacks that the other types face with. Electrochemical biosensors are easy to handle and offer selective, sensitive, rapid and cost effective analysis [11].

#### **1.1.1.1. Electrochemical Biosensors**

Electrochemical biosensors are based on the generation or consumption of electrochemical species during a biochemical process. As a result of the combination of the sensitivity of electrochemical transducers with the high specificity of biological molecular recognition, electrochemical biosensors provide accurate and sensitive detection platforms. The sensing device couples a biomolecule to an electrode transducer which converts the biological molecular recognition into a useful electrical signal [12]. Although biosensing devices employ a variety of biomolecules, electrochemical detection utilizes mainly enzymes because of their biocatalytic activity and specific binding capabilities [13].

Electrochemical biosensors can have different electron transport mechanisms; the so-called generations (Figure 1.3). The first generation biosensors are mainly oxygen based sensors. In the presence of an enzyme, enzyme and oxygen undergo a reaction to form the products which diffuse to the transducer and causes an electrical response. However, this system has a main drawback that is the dependence on the oxygen

concentration level which is difficult to be kept constant [14]. In order to overcome the problems with the first generation setup, the idea of using artificial electron acceptors is developed in the second generation biosensors [15]. In the second generation system, all substances with lower conversion potential than the electrode potentials can affect the overall signal causing interference effect. Therefore, it is crucial to apply electrode potentials as low as possible. Because of this constraint, the concept of using electroactive electron acceptors has evolved in order to provide enzymes to donate electrons. For this purpose, some artificial electron acceptors with low oxidation potentials, i.e. mediators, were discovered which provided a reduction of interference effects. The working principle of second-generation biosensors involves two steps: the first step is the redox reaction between enzyme and substrate which is re-oxidized by the mediator, and the second step is the oxidation of the mediator by the electrode [7]. In the third generation biosensors, denaturation of the enzymes is considered. In order to prevent inactivation and unfolding, enzymes were directly coupled to the electrode without requiring any mediators. This system has the principle of direct electron transfer in which the redox enzyme acts as an electrocatalyst. The immobilized enzyme catalyzes the production of a specific substrate and the electrons are transferred from the substrate to the electrode or vice versa. In recent years, direct electron transfer has been obtained by different immobilization methods and the surface modification of electrode with various conductive materials [16].

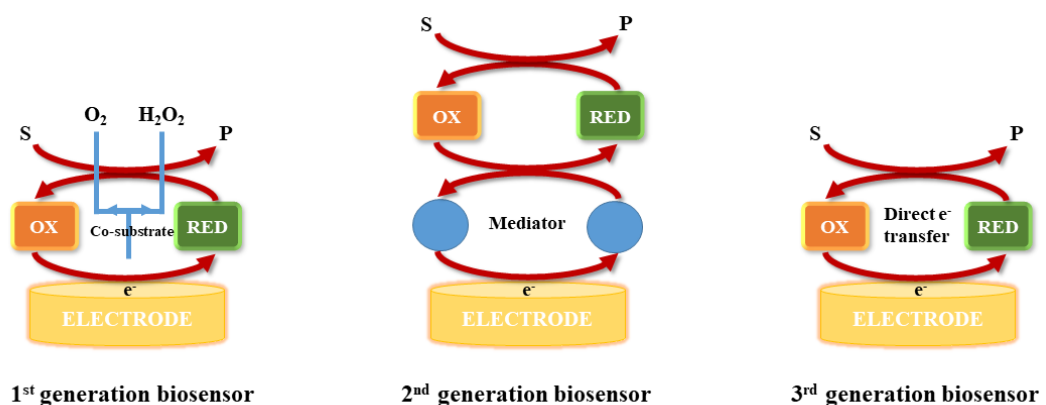


**Figure 1.3.** Working principles of different generations of biosensors

Typically in bio-electrochemistry, the biochemical reaction can either generate a measurable current (amperometric), a measurable potential or charge accumulation (potentiometric) or measurable changes in the conductivity of the reaction medium (conductometric). Therefore, electrochemical detection techniques are generally divided into three main categories of measurement; amperometric, potentiometric and conductometric.

In potentiometric detection, the system measures the potential of an electrochemical cell at the working electrode with respect to the reference electrode when there is zero or negligible current flow between electrodes. The sensor includes an electrochemical cell and measures the potential across a membrane which reacts with the charged ion of interest, selectively. This system can be turned into a biosensor system by coating with a biomolecule catalyzing a reaction which results in the formation of the ion that the electrode is designed to sense. Common potentiometric sensing examples are ion selective electrodes and the glass pH electrode [14].

Conductometric detection is based on the measurement of the changes in conductance between two electrode pairs resulting from a biological element. The working principle is the consumption or generation of charged species as a result of a biochemical process and based on the concentration change of the charged species in the medium which results in a different ionic composition [17].

Amperometric biosensors are based on the measurement of the current produced as a result of electrochemical reduction or oxidation of the electroactive species in the medium upon the application of a constant potential at a working electrode with respect to a reference electrode. The produced current is directly related to the concentration of the electroactive species in the medium. Amperometric biosensors have additional selectivity since the oxidation or reduction potential used for detection is specific for the analyte of interest. Amperometric detection is commonly preferred due to its simplicity and accuracy. Since the fixed potential results in a negligible charging current, that is the current required for the application of the potential to the system, the system minimizes the background signal that adversely affects the limit of detection [18].

Electrochemical biosensors utilize an electrochemical cell with either two or three electrodes. A typical three electrode system consists of a working electrode; a reference electrode, which is usually the silver-silver chloride (Ag/AgCl) electrode, and a counter electrode (Figure 1.4).

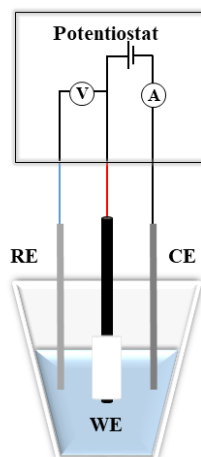


**Figure 1.4.** A typical three electrode electrochemical cell configuration

The counter and working electrodes should be chemically stable, solid and conductive such as, platinum, gold and carbon depending on the analyte. The reference electrode maintains a stable and known potential. The counter electrode provides a connection to the electrolyte solution and it passes all the current needed to balance the current observed at the working electrode. The working electrode serves as the transduction part in the biochemical process. The most important advantage of the three electrode system is that the charge from electrochemical process passes through the counter electrode instead of the reference electrode, which provides the reference electrode to maintain its half-cell potential [18]. A two electrode system includes only the reference and working electrodes. If the current density is low enough, the reference electrode can carry the charge without any adverse effect [19]. Therefore, the two electrode system is generally preferred for disposable sensors because long-term stability of the reference electrode is not essential in these cases.

### 1.1.2. Immobilization Techniques

The biological component must be attached to the electrode surfaces properly and it should preserve its activity for a long time in order to make a convenient and applicable biosensor. The term immobilization accounts for the physical restriction of biomolecules on a specific area while protecting and maintaining the catalytic activities. The immobilization of biomolecules allows the recovery of the costly biomolecules which in turn provides a simplification of the analytical devices [20]. Therefore, effective enzyme immobilization while maintaining free diffusion of substrates and products is the most critical step in enzymatic biosensor preparation. For an effective immobilization, enzyme must maintain its activity, it should be compatible and inert towards host structures and be easily accessible after immobilization. Different immobilization methods have been developed for various systems. Figure 1.5 shows the basic four immobilization strategies; physical adsorption, covalent binding, entrapment and cross-linking.

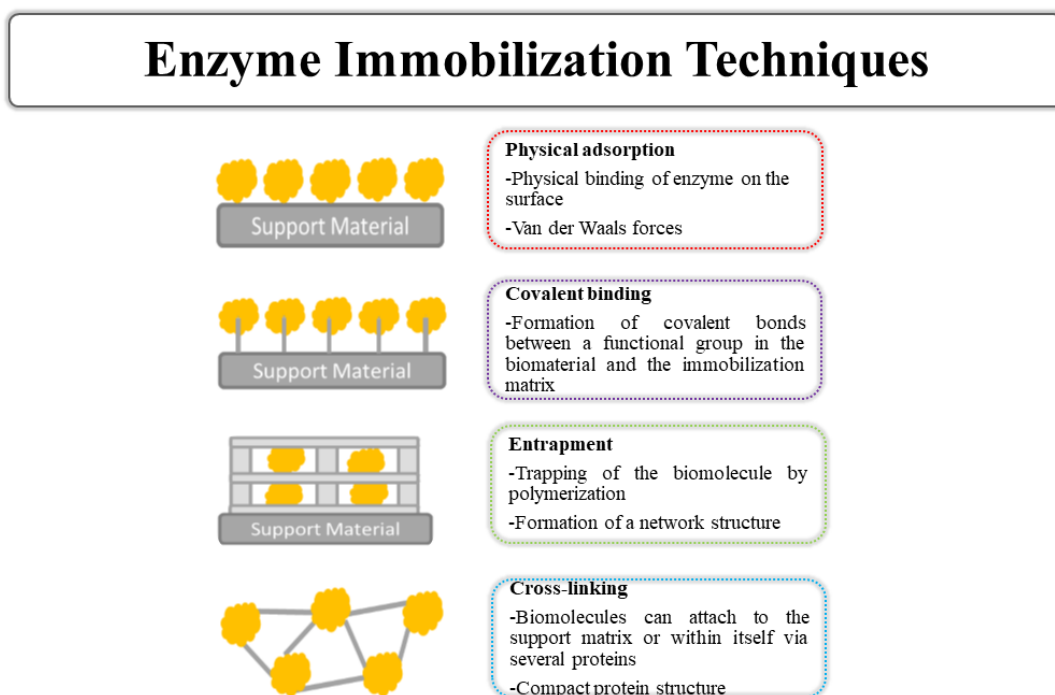


Figure 1.5. Enzyme immobilization techniques

### **1.1.2.1. Physical Adsorption**

Physical adsorption is the simplest and fastest way of immobilization which is mainly provided by creation of physical interactions [21]. For the immobilization, enzyme is dissolved in a solution and it is placed onto the solid support surface for a fixed period of time. Any non-adsorbed enzyme molecules are then removed via washing with either a buffer or distilled water. The adsorption principle is based on weak physical bonds such as Van der Waal's interactions, electrostatic forces, hydrogen bonding and hydrophobic interactions. In general, physical adsorption does not possess any destructive effects to enzyme activity and does not require any functionalization of the surface.

A major advantage of adsorption is that there is no need for reagents or activation steps. In addition, adsorption is less destructive due to the weak physical forces. Although this method does not give rise to enzyme inactivation, it presents some drawbacks. Firstly, since enzymes are loosely bound to the support, the binding forces are affected strongly by pH, temperature and ionic strength changes resulting in desorption of enzymes. Thus, biosensors may suffer from poor storage and operational stability. Moreover, non-specific adsorption of other proteins or substances can occur via this method [22]. Another drawback is the limitation of adsorption to the monolayer of the surface causing immobilization of only a small amount of the enzyme to the surface and since it lies on the outer surface of the support material, it may leach into the sample solution during the measurements [7].

### **1.1.2.2. Covalent Binding**

Covalent binding involves the formation of covalent bonds between a functional group in the biomolecule and the immobilization matrix. This technique mainly occurs via bond formation between the amino acid side chains and the functionalized support surface. Covalent binding is achieved by a two-step process; surface coating with a functionalized support material followed by the coupling of the enzyme having activated functional groups to this active support [23]. Surface functionalization can be achieved via either using a functionalized support material such as polymers,

nanomaterials and macrostructures or activating the surface for covalent coupling. At this stage, activation agents, i.e. linkers, provide enzyme to form covalent bonds to the activated surface via free to attach amino and carboxylic acid groups present in the enzyme structure.

Covalent binding is advantageous since there is a strong and efficient binding between the enzyme and the support surface which can overcome the drawbacks of other weak adsorption techniques. With this method, diffusion limitations and enzyme leaching problems can be reduced. Also, covalent binding facilitates high enzyme stability during biosensor fabrication resulting in increased lifetime stability [24]. However, the main disadvantage of this technique is the possibility of denaturation as a result of excess attachment of enzymes which may result in the loss of bioactivity and instable biosensor construction.

### **1.1.2.3. Entrapment**

Entrapment is the trapping of enzymes by covalent or noncovalent bonds within three-dimensional support matrices such as electropolymerized films, carbon pastes, silica gels or dialysis membranes [25]. In this technique, enzyme, surface material and other additives are deposited onto the sensing layer simultaneously [26].

Since there is no need for biomolecule modification, biosensors fabricated via enzyme entrapment are characterized by high storage and operational stability. However, the major limitation of this method is the performance restriction due to possible diffusion barriers caused by entrapped materials. Moreover, sufficient network pore size should be provided since only appropriately sized substrates and products can diffuse across to provide transformation in a continuous way [22]. Otherwise, leaching of small sized molecules causes inaccurate biosensor responses. Therefore, this method can be applied only to selective enzyme systems. The diffusional barriers also result in long response times since the entrapped enzyme is no longer easily accessible [27].

#### **1.1.2.4. Cross linking**

Cross linking is the joining of the enzyme molecules either to each other to form a large, three-dimensional complex structure or to the surface matrix. The technique allows formation of multiple covalent bonds between enzyme molecules via bi- or multi-functional reagents which results in a compact three-dimensional protein network providing limited leaching of the enzyme from the surface as well as fast response times [22]. Multifunctional reagents can be used not only to link enzyme molecules to each other but also to link them to the support matrices.

However, intramolecular cross linking of enzymes does not provide an effective immobilization to the support matrices unless it is used in conjunction with other immobilization procedures described [28]. The major drawback of this method is the difficulty in controlling the reaction which may cause activity losses due to the distortion of the active enzyme conformation because excess cross linking may result in the chemical alterations of the active site of enzymes [22]. Therefore, it is essential to determine the optimum cross linker amount in order to fabricate a biosensor with a good operational and storage stability.

Among many available cross linkers, glutaraldehyde (GA) has found the widest application in numerous fields. The success of GA as a crosslinker has evolved from its multicomponent nature, where several forms are present in equilibrium at a given pH. Around neutral pH values, it reacts rapidly with amine groups and provides more stable cross links when compared to other aldehydes. In addition to its high reactivity, due to its commercial availability and low cost, GA has had a major role among cross linkers. With the use of GA, immobilization can be achieved for many enzymes under a wide range of conditions [29]. In brief, high cross linking activity of GA results in enhanced immobilization due to improved compact structure of enzymes provided by proper enzyme conformation [30].

### 1.1.3. Glucose Biosensors

Despite the tremendous advances in biosensor technology and their development for the detection of numerous products, glucose biosensors still account for approximately 85% of the current world biosensor market [31]. This can be attributed to the fact that glucose is one of the most essential compounds for life among the biological compounds of nature. Glucose is a sugar derived from the carbohydrate digestion. It passes into the bloodstream and is circulated along the body. Glucose is essential for the energy production required for reproduction and growth processes since it is the primary fuel for glycolysis and anaerobic and aerobic respiration pathways [32]. The regulatory hormone, insulin, which is produced by the pancreas is responsible for maintaining blood glucose levels. When the body fails in insulin production, *Diabetes mellitus*, a metabolic disorder due to insulin deficiency and hyperglycemia, emerges. This disorder is reflected by blood glucose concentrations higher or lower than the normal range. It requires a tight monitoring of blood glucose levels for diagnosis and treatment and millions of diabetics test their blood glucose levels daily [33]. Moreover, in plants, photosynthesis leads to glucose production. The produced glucose is then condensed into starch which is stored as an energy source, or used for the synthesis of numerous saccharides such as cellulose and sucrose. Especially in plant-derived foods, these carbohydrate derivatives assist to flavor and texture as well as serves as a secondary energy consumption source [34].

All of these factors make glucose detection is of great importance in a variety of fields ranging from biomedical applications to ecological approaches. Therefore, concerns related to glucose detection, especially for the diagnostics of diabetes, have led to the development of innovative detection technologies. Among them, amperometric glucose biosensors have had a leading role since they can provide the opportunity of easy-to-use blood glucose testing. Amperometric biosensor technology with a lot of advantages is expected to protect its leading role in continuous glucose monitoring [35].

### 1.1.3.1. Glucose oxidase enzyme (GOx)

For glucose biosensors, GOx is the standard enzyme having a high glucose selectivity. It is easy to obtain, cheap and can work under a wide range of different pH, ionic strength and temperature conditions. The most commonly used from *Aspergillus Niger* has a pH range of 4-7. It is a homodimeric enzyme that catalyzes the conversion of  $\beta$ -D-glucose to D-glucono-1, 5-lactone which subsequently hydrolyzes to gluconic acid spontaneously. Each subunit of GOx needs a redox cofactor, flavin adenine dinucleotide (FAD), and contains one iron atom for catalytic activity [34].

FAD is the initial electron acceptor in the catalytic reaction and is reduced to FADH<sub>2</sub> which reacts with oxygen and results in regeneration of the cofactor and hydrogen peroxide formation [36]. The reaction mechanism of GOx is shown in Figure 1.6. Because of the production of electroactive H<sub>2</sub>O<sub>2</sub>, GOx reactions can be utilized in lots of the glucose detection systems. Oxidation of H<sub>2</sub>O<sub>2</sub> allows the electrode to recognize the number of transferred electrons which is proportional to the glucose concentration. For the electrochemical glucose monitoring, three general methodologies; oxygen consumption monitoring, detection of the produced hydrogen peroxide amount and use of a mediator for the electron transfer from the GOx to the electrode can be utilized [37].

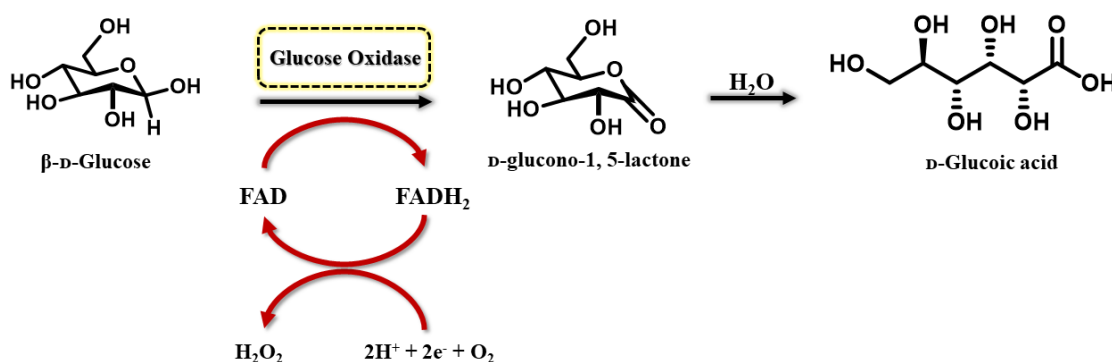


**Figure 1.6.** Glucose oxidase reaction mechanism

## 1.2. Conjugated Polymers (CPs)

At the end of 1970s, the investigation of highly conductive poly(acetylene) in its doped state has started a new era in the field of polymer technology. In 1967, when Shirakawa and coworkers performed the synthesis of polyacetylene using tremendous amount of Ziegler-Natta catalyst accidentally, they produced a thin silvery semiconductor film with a drastic change in the conductivity of the polymer upon halogen addition [38]–[43]. Among scientist, this investigation evoked the awareness that an insulator polymer can be converted to a semiconductor and a metallic form.

The discovery of conducting polymers brought Alan MacDiarmid, Alan Heeger and Hideki Shirakawa the Nobel Prize in Chemistry in 2000 which opens up the field of “plastic electronics”. This innovative discovery brought about new application areas combining known characteristics of polymers with high electrical conductivity.

Conducting polymers, i.e. conjugated polymers (CPs), are organic polymers with the ability to conduct electricity. They contain extended  $\pi$ -conjugated system having alternating single and double bonds along the polymer chain. In other words, the backbone of CPs contains continuous  $sp^2$  hybridized carbon centers and the orbitals of these successive carbon atoms overlap providing delocalization of electrons along the polymer backbone which results in charge mobility [44].

The  $\pi$ -conjugated system is the major factor that is responsible for the promising electronic properties of CPs such as conductivity, high electron affinity, low ionization potential and low energy optical transitions making them as an important class of materials for electronic, optoelectronic and biotechnological applications. One of the major advantages of CPs is their processability allowing simple modifications on their chemical structure in order to obtain the required electrochemical properties [45].

### 1.2.1. Theory of Conjugated Polymers

The electronic structure and conduction mechanism of materials can be explained by the band theory which is based on the overlap of orbitals to form delocalized energy bands. The conductivity of a material is related to the relative population of each band

and the energy difference between them [46]. According to their conductivity properties explained by the energy diagrams, materials can be defined as insulators, semiconductors and metals (Figure 1.7). The theory names the highest occupied molecular orbital (HOMO) as the valence band and the lowest unoccupied molecular orbital (LUMO) as the conduction band and the energy difference between these bands is known as the band gap ( $E_g$ ) which determines the motion of electrons. While the band gap of an insulator is too large for electron transfer, the absence of any energy gap aids the electron flow, thus high conductivity in a metal. On the other hand, a semiconductor has a filled valence band and an empty conduction band with a narrow band gap.

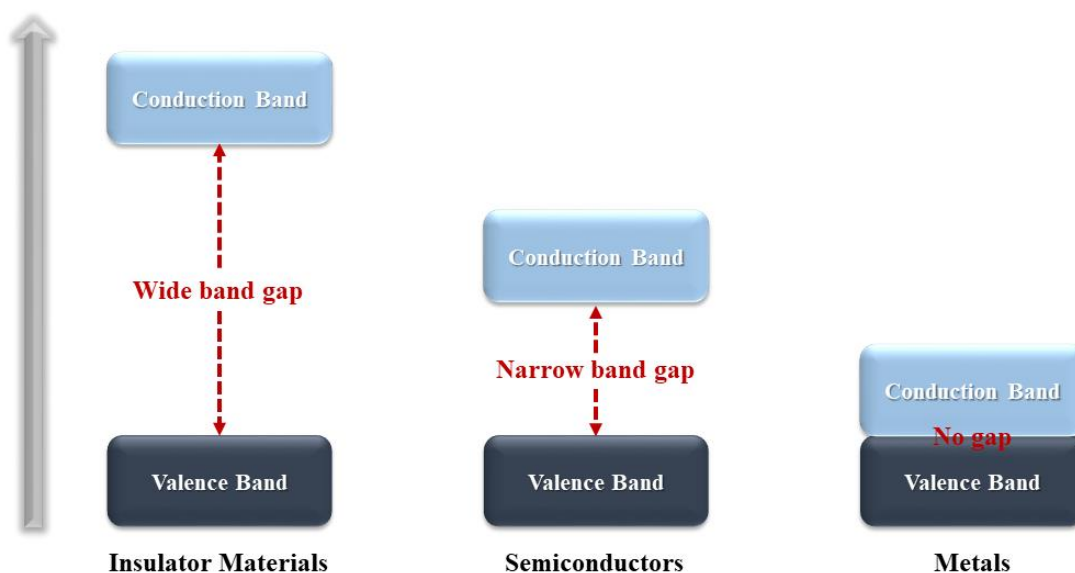


**Figure 1.7.** Band structures of insulator materials, semiconductors and metals

It is possible, however, to increase the conductivity of semiconductor materials upon doping process with charge carriers. It can be performed either by taking electrons from the valence band and creating holes via p-type doping or adding electrons to the conduction band via n-type doping [47].

Electron flow, which is the main concept of conductivity, can be possible in CPs since the electrons are loosely bound in a conjugated system.  $\pi$ -bonds are included in each

double bond and they are not strongly localized resulting in a weaker bond which is the main reason of electron delocalization in a conjugated system resulting in the movement of electrons. However, only the presence of conjugation is not enough for conductivity of a polymeric material. The polymer also needs to be doped to provide electron flow. Doping process that is used for the conductivity enhancement of a polymer is a redox process involving electron reduction or oxidation on the polymer backbone. It can be performed via either chemical or electrochemical procedures. When the polymer is doped, the electrons in the  $\pi$ -bonds become able to jump around the polymer backbone bringing about electric current [48]. The conductivity of CPs can be manipulated by the nature of the dopant, by chemical modifications on the polymer backbone to change the band gap of the material, by blending with other polymers and by the degree of doping [49].

### **1.2.2. Conjugated Polymers in Biosensor Applications**

Since the discovery of CPs, plastic electronics have opened innovative research in a lot of scientific and technological areas due to their tremendously attractive properties. In addition to their excellent metal-like conductivity, they possess high mechanical strength and processability like polymers. Moreover, the chemical nature of CPs and the facile methods to synthesize and modify them make them compatible with many of the chemistries found in nature [50]. Therefore, they have become as potential material candidates for a wide range of applications such as sensors, electrochromic and photovoltaic devices, storage batteries, ion-specific membranes, electroluminescence and drug delivery [51].

For biosensor applications, CPs have become an important class of materials for surface design since they provide enhanced stability, sensitivity, versatility and fast response. One of the biggest advantages of CPs for biosensors is that they provide a suitable matrix for biomolecules immobilization and preserve their activity for a long time. Furthermore, they can act as transducers since they have the ability to transfer the electric charge generated by the biochemical reaction to the electric circuit. Their flexible chemical structures provide easy modification according the desired

electronic and mechanical properties. Additionally, the polymer itself can be modified to bind the biomolecule. Moreover, CPs exhibit exchange and size exclusion properties since they are very sensitive and specific to the desired analytes [52]. As a result, CP-modified electrodes have opened a new area in the design of biosensors that allow reliable, simple, accurate and low-cost determination of numerous analytes.

### **1.3. Carbon Nanotubes (CNTs)**

The innovative discovery of fullerenes provided exciting perceptions into carbon nanostructures with the most striking example of carbon nanotubes. Quasi-one-dimensional carbon nanotubes are perfectly straight tubular structures having nanometer size diameters and they possess characteristics of an almost ideal graphite fiber. In 1991, their incidental discovery by Sumio Iijima occurred when the scientist was studying the graphite electrode surfaces used in an electric arc discharge, and the observation of these tubular structure developed a new perspective in the carbon research. The topology, structure and size of CNTs are the properties making them much more exciting compared to the other graphite related structures [53]. CNTs are well-ordered, tubular graphitic nanostructures that are made of  $sp^2$ -hybridized carbon atom cylinders. They can be imagined as hollow tubes that take the shape of rolled graphite sheets. According to the number of rolled graphite sheets, they can be divided into single-walled carbon nanotubes (SWCNTs) and multi-walled carbon nanotubes (MWCNTs) (Figure 1.8). SWCNTs are single molecular nanomaterials formed from a single sheet of graphite, i.e. graphene; while MWCNTs are composed of more than two layers of graphite sheets. The diameter of SWCNTs is in the range of 0.75-3 nm and the length is about 1-50  $\mu\text{m}$ . For MWCNTs, the diameter is in the range of 2-30 nm, some can be more than 100 nm, and the distance between each layer is about 0.42 nm [54].

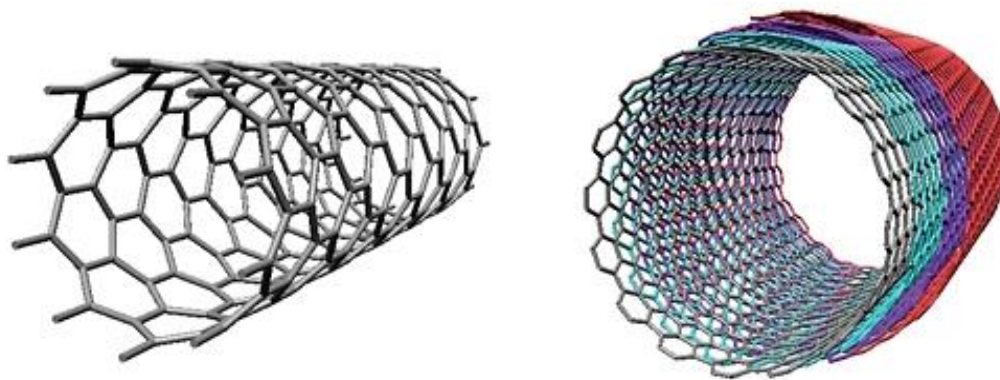


**Figure 1.8.** Carbon nanotubes: single-walled carbon nanotubes (SWCNTs) on the left; and multi-walled carbon nanotubes (MWCNTs) on the right.

Since their discovery, CNTs have quickly emerged as a global research area which is mainly because of their tremendously high specific surface area and superior mechanical, electrical and electrochemical properties.

### **1.3.1. Carbon Nanotubes in Biosensor Applications**

Outstanding electrochemical properties of CNTs have opened a field for their use as surface platforms in the construction of biosensors. They combine exceptional chemical, physical, optical and electronic characteristics making them well-suited materials for the signal transduction related with analyte recognition [55].

Studies have proven that CNTs have the ability to enhance the electrochemical reactivity of biomolecules, and can promote the charge transfer in biochemical reactions. In this respect, CNTs are attractive especially for oxidase- and dehydrogenase based enzyme electrodes. Many of these enzymes specifically catalyze the reactions of analytes and generate the electrochemically detectable Nicotinamide adenine dinucleotide (NADH) and hydrogen peroxide products whose electrochemical reactivity are enhanced by CNTs making them very promising nanomaterials for fabricating electrochemical biosensors providing easy detection of biomolecules [56].

In addition to providing enhanced electrochemical reactivity, CNT-modified electrodes are attractive structures for the accumulation of biomolecules since their hollow core is a suitable host structure for supporting the guest biomolecules. Also, CNTs have the largest elastic modulus of any known material [56].

The high surface-to-volume ratio of the CNTs contributes to biomolecular conjugation. In this way, the immobilized enzyme on CNTs can protect its biological activity and stability. Moreover, the easy modification of CNTs by attaching almost any desired moieties allows very fast detection of biomolecules at low concentrations. Therefore, CNT-based biosensors can be the key for ultra-sensitive biosensing systems [57].

Although research has made amazing progress in the field of CNT-based biosensors, there are still some challenges and further works in order to enhance their properties and develop advanced systems. It is a real challenge to protect the thermal stability and lifetime of CNT-based biosensors. Also, CNT-based biosensor systems generally require joint platforms with other supporting materials. Therefore, the development of CNT-based biosensors is a multi-faced challenging work requiring a cooperation between different fields of science.

#### **1.4. Macrostructures in Biosensor Design**

In the performance of electrochemical biosensors, the modification of electrode surfaces has a crucial role since reactions can be detected only in close proximity to the surface. Therefore, the material and dimensions of the electrode, and its surface modification significantly affect its detection ability [14]. In this regard, there are a number of options as supporting materials. In this thesis, utilization of two different macrostructures were studied in addition to conjugated polymer and MWCNTs modification which are well-studied in literature.

### 1.4.1. Phthalocyanines (Pcs)

Since their incident discovery in 1928, Pcs, which are synthetic analogues of the naturally occurring porphyrins, have been utilized in numerous research fields. They are planar 18  $\pi$ -electron aromatic macrocycles consisting of four isoindole units with a considerable large  $\pi$ -delocalized surface that accounts for their unique optical properties (Figure 1.9).

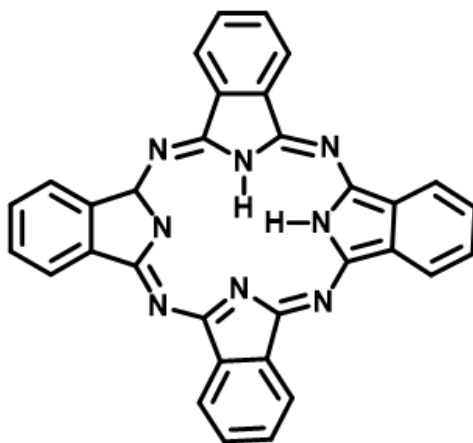


**Figure 1.9.** General structure of phthalocyanines

For many years, due to their dark green-blue color, Pcs have played a significant role in colorants for inks and textiles which is confirmed by their absorption spectra presenting an intense Q-band in the visible region, centered at 620-700 nm [58]. In recent years, they have been realized as attractive materials for molecular and nanotechnological applications and have been successfully incorporated in electrochromic and semiconductor devices, liquid crystal color displays and information storage systems, etc. [59].

Pcs have become outstanding in materials science and nanotechnology because they are thermochemically stable and robust to strong electromagnetic radiations in addition to their electronic and absorption properties. More importantly, Pcs are remarkably versatile since the two hydrogen atoms in the central cavity allow incorporation of different substituents and can be replaced by more than 70 metals.

That is, the structure allows tuning of physical properties. This modification is possible both at the periphery of the structure and at the axial positions. The possible structural modifications can allow the creation of the so-called Pc analogues. Generally, the extension of the  $\pi$ -system, different number of isoindole units and exchange of the isoindole units with other hetero-aromatic ring moieties result in the building of these Pc analogues [60].

Although many Pc derivatives suffer from solubility problems limiting their potential applications, the chemical flexibility of Pcs allows the introduction of suitable substituents that increase their solubility as well as tune their electronic properties. As a result of this versatility, incorporation of Pcs into electro and/or photo active systems is possible via linking with suitable units which in turn enlarges the applicability of this macrostructures.

#### **1.4.1.1. Metal Phthalocyanines (MPcs)**

Pc structures with one or two metal atoms are named as metal phthalocyanines (MPcs). That is, they are cyclic, conjugated organic macrostructures having metal atoms at the center (Figure 1.10). Due to the high versatility of the Pcs, metalation can tune the properties of the structure completely. Together with their unique plane structures, they have been utilized in variety of applications including molecular electronics, optoelectronics, sensors, etc. [61]. Especially for the applications having MPcs as electrocatalysts, MPcs with redox active metal centers is of importance. The emerging functions of MPcs are mainly based on electron transfer reactions resulting from the  $\pi$ -conjugated ring system, interaction of the  $\pi$ -electrons with center metal atoms and the substituents in their structure [62].

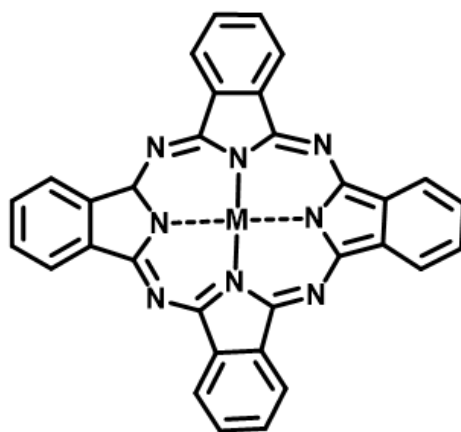


**Figure 1.10.** General structure of metal phthalocyanines

For biosensor applications, MPcs have emerged as promising materials due to their electronic properties, rich redox chemistry and thermo-electrochemical stability. Their electrocatalytic property, low raw material cost and bio-compatibility with a lot of biomolecules provide Pcs to be widely employed as electrode modifiers in biosensor construction [63]. In this regard, a novel water soluble zinc phthalocyanine molecule for electrochemical glucose sensing was utilized in this thesis.

However, since pristine MPcs are adsorbed physically on the electrode surface, they may leach out from the surface causing instability and low reproducibility. In addition, their tendency for aggregation and low electrical conductivity limit their electrochemical performance [64]. In this regard, they required to be supported by suitable materials in order to construct stable electrodes having improved electrochemical properties. Incorporation of Pcs with carbon nanostructures, such as CNTs, appears as a possible way for this purpose [65]. In particular, MWCNTs are promising nanomaterials in this combination since they enhance electrochemical conductivity and facilitate electron transfer of MPcs [66]. Due to their  $\pi$ -conjugated aromatic surface, Pcs have the ability to bind to the side walls of MWCNTs by means of  $\pi$ - $\pi$  interaction resulting in the formation of an improved hybrid system and the protection of the chemical and electronic structure of MWCNTs [67].

In this context, a novel ZnPc molecule have been synthesized in order to investigate the role of being a part of active layer in biosensor construction. Introduction of tetra quaternized imidazolyl moieties at the peripheral positions of Pc structure resulted in high solubility in water. Immobilization platform was constructed via incorporation of ZnPc with MWCNTs into the CP matrix on a graphite electrode surface.

#### **1.4.2. Dendrimers**

Dendrimers, originally referred to as cascade molecules and arborols, are highly symmetrical and branched structures being the most recently identified members of the polymer family. The first reports about dendrimers were published in the late 1970s and early 1980s by the research groups of Vögtle [68], Denkewalter [69], Tomalia [70] and Newkome [71]. After these pioneering publications, the research in this field attracted great interest and proceeded rapidly.

Ideally, dendrimers are perfectly monodispersed macrostructures having a regular and highly branched three-dimensional pattern with a very high density of surface functional groups. These structures are formed from a core, and expand with each subsequent branching moiety. In the structure of dendrimers, dendron is the remaining part when the core is removed and the number of dendrons is dependent on the multiplicity of the core. A dendron can be divided into three regions; the core, the branches (interior) and the end groups (periphery). The number of branch points from the core to the periphery of a dendron defines its generation (G1, G2, G3, etc.) with higher generation dendrimers being larger, more branched and having more end groups (Figure 1.11) [72]. The internal space between the branches of a dendrimer forms cavities which are named as dendrimeric crevices. The properties of dendrimers are mainly directed by peripheral functional groups, yet the functionality of the cavity and the core are also of great importance. They are generated in a repetitive reaction sequences in which each additional repeat results in a higher generation structure [73].

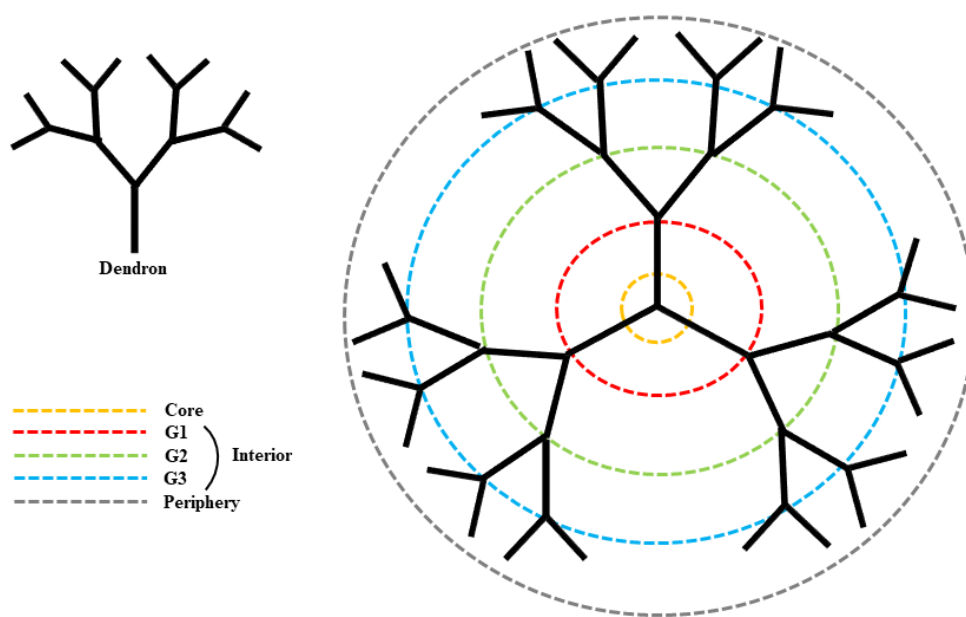


**Figure 1.11.** Anatomy of a dendrimer

Since dendrimers have a specific molecular weight, unique branched topologies and definite size and shape, they emerged as promising materials for numerous applications. Their high conformational flexibility brings about many initially unexpected properties. The flexible nature of dendrimer branches can adopt different conformations, causing the end groups to be folded back into the interior part of the structure. In higher generations, the flexibility allows these molecules to adopt shapes that are far from globular. In addition, multivalency of dendrimers may be their mostly utilized property since it can significantly affect the solubility properties and many of the proposed uses of dendrimers rely on the presence of large amount of end groups [74].

Multiple conjugation sites of the dendrimers provide a densely functionalized and stable structure. Also, the available interior void space of dendrimers helps to prevent diffusional restriction for analytes and electron-transfer reagents which allow the biochemical processes throughout whole range of multilayers [75]. Furthermore, the exciting properties of dendrimers, especially their controllable size, globular

geometry, hydrophilicity, high surface functionality and stability make them as ideal matrices for biosensor applications since these properties provide better sensitivity, target capturing ability, specificity, reusability and stability [76].

#### **1.4.2.1. Poly(amidoamine) (PAMAM)**

Within the family of dendrimers, globular-shaped PAMAM dendrimers are the first and the mostly studied structures. In recent years, numerous studies demonstrated that PAMAM dendrimers can be utilized as bio-conjugating reagents for construction of biosensing devices. These highly-branched dendritic macromolecules can be used in biosensor applications since they contain a number of terminal amino groups which enhances the attachment of biomolecules (Figure 1.12). Moreover, their good biocompatibility and functional groups for chemical attachment make PAMAM dendrimers as promising electrode modifiers [77].

As the density of the terminal amino groups on the surface increases, the generation of PAMAM dendrimer grows and affects the biomolecule attachment depending on the electrode surface design. PAMAM G2 and G4 moieties possess 16 and 64 primary amine groups on their surface, respectively. The presence of these multiple functional groups allows multiple interactions and conjugations with biomolecules resulting in enhanced stability [78]. Hence, the lifetime of the sensing device increases.

However, direct attachment of dendrimers onto the surface is not easy since they are oily liquids. Moreover, dendrimers can decrease the conductivity of the modified probe, resulting in a lower detection sensitivity which limits their applications in biosensors [79], [80]. In order to overcome these problems, the present study aimed to enhance the sensitivity of the dendrimer attached probe with the addition of MWCNTs and increase the stability with CP modification.

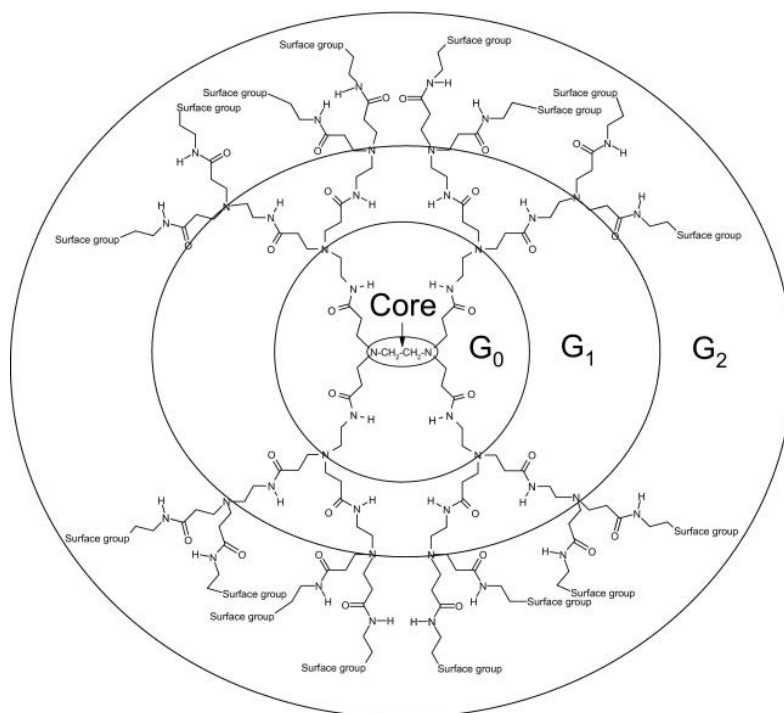


**Figure 1.12.** Structure of PAMAM dendrimers

### 1.5. Aim of This Thesis

In this thesis, two different conjugated polymer based amperometric biosensors were designed with the utilization of different macrostructures in order to investigate the effects of these structures on biosensor performance. The fabricated sensing systems were used in glucose detection.

For this purpose, in the first study, ZnPc molecule was utilized in combination with MWCNTs in the CP based sensor design. Following the surface modification of graphite electrode with these structures, GOx immobilization was performed via physical adsorption and using GA as the crosslinker. CP provided a stable immobilization platform due to the strong  $\pi$ -interactions with the enzyme molecule. MWCNTs enhanced the charge transfer rate and made the immobilization more durable due to the high mechanical and chemical strength of the structure. By taking the high stability, rich redox and electronic properties of ZnPc structure, biosensor performance was enhanced.

In the second study, the same CP was combined with PAMAM dendrimer and MWCNTs. After the modification of the graphite electrode surface with these supporting materials, GOx was immobilized via physical adsorption and using GA as the crosslinker. Here, the CP and MWCNTs were used due to their above-mentioned properties. PAMAM dendrimer was chosen as the additional modification material since it is a suitable host structure for accommodation of the guest enzyme molecule due to its three-dimensional structure with an internal void space as well as since it contains a number of terminal amino groups which enhances the attachment of the enzyme molecule.

Both of the fabricated biosensors were optimized, characterized and applied for real-time analyses in order to make a contribution to the field of surface design for the electrochemical biosensors via developing novel surface architectures.



## CHAPTER 2

### PFLA/ZnPc/MWCNTs/GOx BIOSENSOR

#### 2.1. Experimental

##### 2.1.1. Materials and Methods

Glucose oxidase (GOx,  $\beta$ -D-glucose: oxygen 1-oxidoreductase, EC1.1.3.4, 17300 units/g solid) from *Aspergillus niger* and D-glucose were purchased from Sigma (St. Louis, USA). Glutaraldehyde (GA), multi walled carbon nanotubes (MWCNTs) and chloroform were obtained from Sigma–Aldrich Co., LCC. (St. Louis, USA). Dimethylformamide (DMF) was purchased from Carlo Erba Reagents SAS (Reuil, France). The polymer, poly[9,9-di-(2-ethylhexyl)-fluorenyl-2,7-diyl] end capped with N,N-bis(4- methylphenyl)-4-aniline, (PFLA) was obtained from American Dye Source, Inc. (Quebec, Canada). For enzyme immobilization, a 50 mM, pH 7.0 phosphate buffer solution (PBS) consisting of 0.025 M Na<sub>2</sub>HPO<sub>4</sub> (Fisher Scientific Company) and 0.025 M NaH<sub>2</sub>PO<sub>4</sub> (Fisher Scientific Company) was used. As the substrate, glucose solution (0.1 M) was prepared by dissolving 0.18 g of glucose in 10 mL pH 7.0 PBS solution. All chemicals were of analytical reagent grade.

All the amperometric measurements and cyclic voltammetry studies were conducted using PalmSens potentiostat (PalmSens, Houten, The Netherlands). Three electrode system consisting of a graphite rod working electrode (Ringsdorff Werke GmbH, Bonn, Germany, typeRW001, 3.05 mm diameter and 13% porosity), Pt wire counter electrode (Metrohm, Switzerland) and Ag wire reference electrode was used for all electrochemical studies. Scanning electron microscope (SEM) (JEOL JSM-6400 model) was used for the surface modification characterization of the fabricated biosensor. All measurements were conducted at ambient conditions.

### 2.1.2. Preparation of the Biosensor

Before surface modification, spectroscopic grade graphite rods were polished on emery paper and washed with distilled water. CP solution was prepared by dissolving 2.0 mg PFLA in 2.0 mL chloroform and a 10  $\mu$ L aliquots from this solution were deposited on a cleaned graphite electrode surface. Then, MWCNTs suspension was prepared by dispersing 0.5 mg MWCNTs in 10 mL DMF followed by 15 min ultrasonication to obtain a black suspension. After the CP modified electrode was dried at ambient conditions, 10  $\mu$ L aliquots of the prepared MWCNTs solution were cast on the electrode surface and the electrode was left to dry at room temperature for 3 h. Then, ZnPc solution was prepared as 1.0 mg of ZnPc in 1.0 mL distilled water. For the co-immobilization of GOx and ZnPc, the certain amount of GOx was dissolved in 3.0  $\mu$ L of PBS (50 mM, pH 7.0) and 3.0  $\mu$ L of the prepared ZnPc solution were mixed with this solution. 6.0  $\mu$ L of the mixture was co-immobilized on the modified electrode surface followed by the addition of 3.0  $\mu$ L of GA crosslinking solution (1% in 50 mM PBS pH 7.0) to the electrode surface. After the prepared electrode was left to dry for 2 h at ambient conditions, the fabricated biosensor was rinsed with distilled water to remove the unbound molecules and impurities. Figure 2.1 illustrates schematic representation of the procedure for the construction of the proposed biosensor.

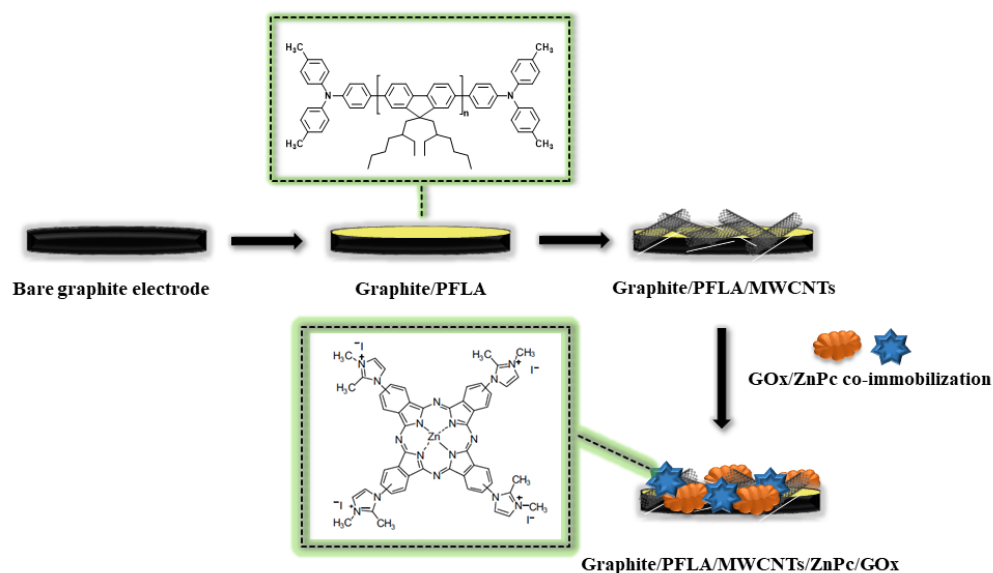


**Figure 2.1.** Schematic representation of PFLA/MWCNTs/ZnPc/GOx Biosensor

### 2.1.3. Amperometric Measurements

All amperometric studies were performed in a reaction cell filled with 10 mL pH 7.0 PBS solution by applying -0.7 V constant potential at ambient conditions under mild stirring. As a result of the enzymatic reaction between GOx and the substrate, the decrease in the oxygen level associated with substrate concentration was monitored at -0.7 V potential since the response of the biosensor for this reaction is most sensitive at this potential [81]. During the amperometric measurements, when the baseline current reached to an equilibrium, certain amount of glucose substrate was added into the reaction medium. As a result of the enzymatic reaction between GOx and the substrate, the current changed and a new equilibrium was established. The difference between these two constant current values ( $\mu\text{A}$ ) gave the biosensor response (Figure 2.2). The buffer solution was refreshed and the electrodes were washed with distilled water, then kept in buffer solutions for a while after each measurement. In all amperometric studies, each measurement was carried out three times repetitively and the data were given as the average of these measurements and standard deviations were recorded as  $\pm\text{SD}$ .

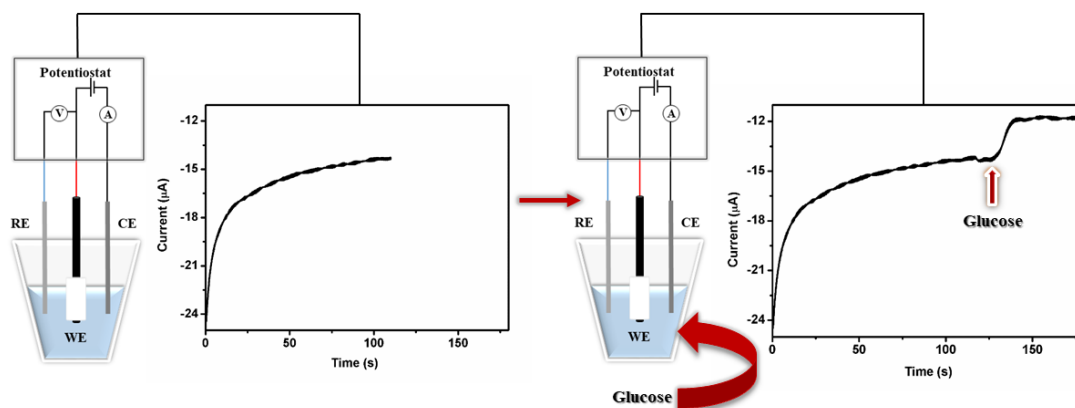


**Figure 2.2.** Amperometric measurement procedure

### 2.1.4. Optimization of Biosensor Performance

It is aimed to achieve a long life and robust biosensor for the analyte detection in the design of enzyme based biosensors. For this purpose, all the parameters affecting the biosensor performance in the construction were optimized in order to obtain a stable

and reproducible biosensor response. Therefore, in this study, the effects of different amounts of CP, MWCNTs and ZnPc as well as enzyme concentration and pH values on the current signal were investigated. In order to perform the optimization studies, different electrodes were prepared by changing only the amount of the parameter to be optimized. In other words, the amounts of all the other parameters were kept constant except for the one to be optimized and the performances of the different electrodes were compared. The one with the highest signal was chosen as the optimum value and used for the biosensor construction at further steps.

Moreover, in order to achieve the best combination for the highest biosensor performance, different biosensors were prepared as different combinations of PFLA, MWCNT and ZnPc with their optimized parameters. The corresponding responses of these combinations were compared to determine the best surface design.

## **2.1.5. Characterizations**

### **2.1.5.1. Analytical and Kinetic Characterizations**

After all optimum conditions for the proposed biosensor were determined, a calibration curve for glucose was plotted. The analytical parameters, limit of detection (LOD) and sensitivity values, were calculated by setting the intercept of the linear range of the calibration curve to zero using  $S/N$  (signal-to-noise ratio) = 3 criterion. Moreover, in order to prove the repeatability of the proposed sensing system, 10 consecutive measurements were done for 0.5 mM glucose solution. The standard deviation (SD) and the relative standard deviation (RSD) values were calculated for these measurements. The shelf life of the biosensor was also measured by taking amperometric measurements with regular time intervals for 30 days. Percent activity loss value was calculated at the end of this time by comparing the average signal of the measurements at the first day and the last day.

For the kinetic characterization of the biosensor, Michaelis-Menten enzyme kinetics model was used. It is known that  $V_{\max}$  or  $I_{\max}$  and  $K_M$  are the parameters that characterize the kinetics of biochemical reactions. Michaelis-Menten model utilizes

an equation to describe the relation between the rates of an enzymatic reaction to the substrate concentration, i.e. [S]. The reaction rate gradually increases as [S] increases, but as [S] gets higher, enzyme becomes saturated with the substrate and reaction rate reaches its maximum value,  $V_{max}$ . Half of the maximum velocity is called  $K_M$ , Michaelis constant, which is a measure of enzyme affinity to its substrate [82], [83].

Michaelis-Menten equation; 
$$v = \frac{V_{max}[S]}{K_M + [S]}$$

Since the Michaelis-Menten plot,  $v$  vs [S] is not linear, its linear form Lineweaver-Burk plot is used to obtain  $I_{max}$  and  $K_M^{app}$  values.

Lineweaver-Burk equation; 
$$\frac{1}{v} = \left(\frac{K_M}{V_{max}}\right) \frac{1}{[S]} + \frac{1}{V_{max}}$$

Since the studies were conducted as amperometric method which measures the current change with respect to time,  $I_{max}$  and  $K_M^{app}$  values were calculated from Lineweaver-Burk plot ( $1/I$  vs  $1/[S]$ ).

#### 2.1.5.2. Surface Characterizations

Cyclic voltammetry (CV) studies were carried out to characterize the effective electroactive surface area for each modification. Experiments were performed in a solution containing 5.0 mM  $\text{Fe}(\text{CN})_6^{3-/4-}$ , 0.1 M KCl and 50.0 mM PBS pH 7.0 by applying the potential between 0 and 1.0 V with a scan rate of 100  $\text{mV s}^{-1}$ . Determination of electroactive surface areas for each surface modification was performed using Randles-Sevcik equation:  $I_p = 2.69 \times 10^5 A D^{1/2} n^{3/2} V^{1/2} C$  where  $n$  is the number of electrons involved in the redox reaction,  $A$  is the electrode area ( $\text{cm}^2$ ),  $D$  is the diffusion coefficient of the molecule in solution ( $\text{cm}^2 \text{s}^{-1}$ ),  $C$  is the concentration of the probe molecule in the bulk solution ( $\text{mol cm}^{-3}$ ) and  $V$  is the scan rate ( $\text{Volt s}^{-1}$ ). The equation suggests that there is a direct relation between the peak current and effective surface area. In other words, any increase in the peak current means a proportional increase in the electroactive surface area.

Moreover, SEM technique was used for surface morphology characterization for different surface modifications. Images of pristine PFLA, PFLA/MWCNTs/ZnPc and PFLA/MWCNTs/ZnPc/GOx modified electrode surfaces were analyzed.

#### **2.1.6. Sample Application**

In order to validate the reliability of the sensing system, the biosensor was tested for glucose detection on several commercially available beverage samples. For this purpose, instead of glucose solution, 10  $\mu$ L of beverage samples were directly injected into the reaction cell filled with 10 mL buffer solution. By this way, automatic dilution occurred and the detected concentrations were included in the linear range of the system. The biosensor signals for the beverage samples were recorded and the glucose contents were calculated from the equation of the calibration curve. The results were compared with the glucose contents given on the product labels and relative error for each sample was calculated.

### **2.2. Results and Discussion**

#### **2.2.1. Optimization Studies**

##### **2.2.1.1. Optimization of the Biosensor Parameters**

Firstly, the effect of different CP concentration on biosensor performance was investigated since unstable and low biosensor responses show up in the case of improper CP amounts. In order to determine the optimum CP concentration; 1.0, 1.5, 2.0, 2.5 and 3.0 mg of PFLA were dissolved in 2.0 mL of chloroform and 10  $\mu$ L aliquots of these solutions were deposited on graphite electrodes. The biosensor responses of corresponding electrodes were compared by keeping all the other parameters constant. The highest biosensor performance was obtained with 2.0 mg PFLA (Figure 2.3).

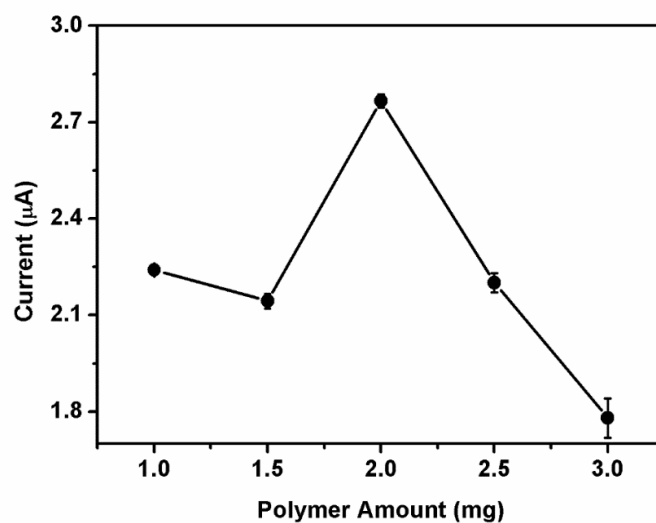


**Figure 2.3.** The effect of polymer amount on biosensor response (in 50.0 mM PBS, pH 7.0, 25°C). Error bars show the standard deviation (SD) of three measurements.

Then, the amount of MWCNTs was optimized since higher amounts of MWCNTs cause lower biosensor responses due to diffusional constraints for the substrate. On the other hand, lower amounts of MWCNTs affect the biosensor performance due to improper fixation problem of enzyme molecules onto electrode surface. In order to find the optimum MWCNTs amount; 0.25, 0.40, 0.50, 0.60, 1.00, 1.50 and 1.75 mg of MWCNTs were dispersed in 10.0 mL of DMF by ultrasonication and 10 µL aliquots of these solutions were cast on the CP coated electrode surfaces. When the recording signals were compared, biosensor with 0.50 mg MWCNT gave the highest response (Figure 2.4).

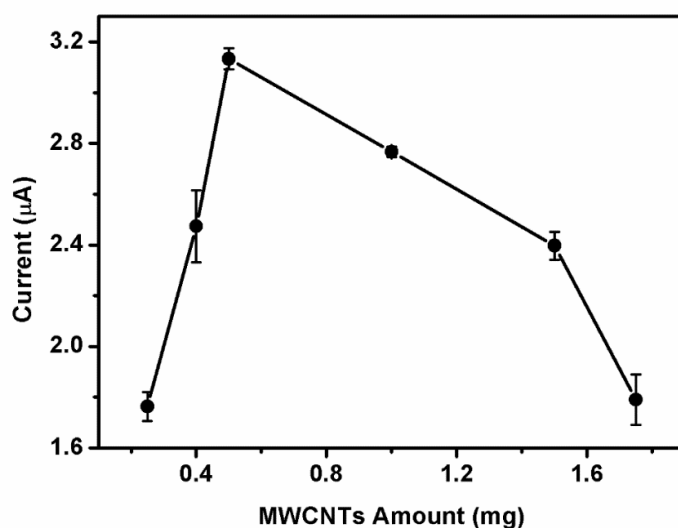


**Figure 2.4.** The effect of MWCNTs amount on biosensor response (in 50.0 mM PBS, pH 7.0, 25°C). Error bars show the standard deviation (SD) of three measurements.

Furthermore, optimum ZnPc amount for the biosensor was also determined. MPC complexes are strongly adsorbed onto carbon-based materials. In addition, since their high stability and superior catalytic properties may enhance biosensor performances, the biosensor signal increases with increasing MPC amount. However, further increase in MPC amounts results in lower signal and sensitivity as a result of increased diffusion constraints. Therefore, in order to determine the optimum ZnPc amount, different solutions were prepared by dissolving 0.25, 0.50, 1.00, 1.50 and 1.75 mg of ZnPc in 1.0 mL of distilled water and 3.0 µL aliquots of these solutions were co-immobilized with GOx solution. When the corresponding signals were examined, 1.00 mg ZnPc resulted in the highest biosensor response (Figure 2.5).

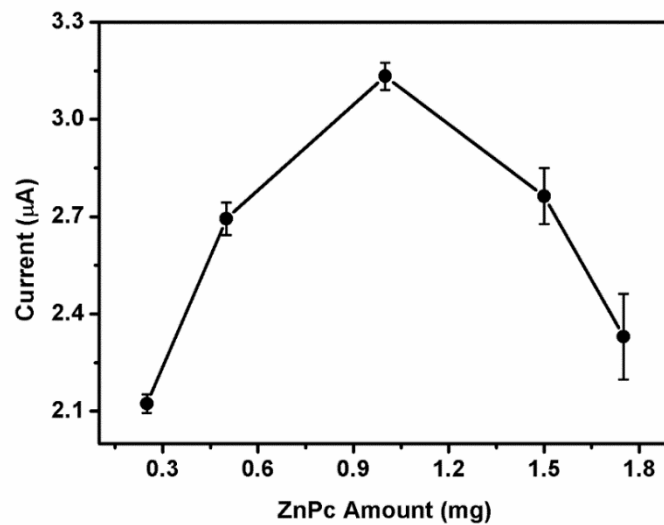


**Figure 2.5.** The effect of ZnPc amount on biosensor response (in 50.0 mM PBS, pH 7.0, 25°C). Error bars show the standard deviation (SD) of three measurements.

Enzyme amount was also optimized to obtain the highest biosensor performance since the immobilization matrix has an enzyme loading capacity. That is, if there is an excess enzyme loading on the electrode surface, the excess amount may leach out from the surface. On the other hand, if the enzyme amount is far below the loading capacity of the surface, the desired responses for better sensitivity cannot be recorded. To optimize the enzyme amount, different electrodes with 0.5 mg (8.7 U), 1.0 mg (17.3 U), 1.3 mg (22.5 U), 1.5 mg (26.0 U) and 2.0 mg (34.6 U) GOx were prepared and the best signal was recorded with 1.3 mg GOx (Figure 2.6).

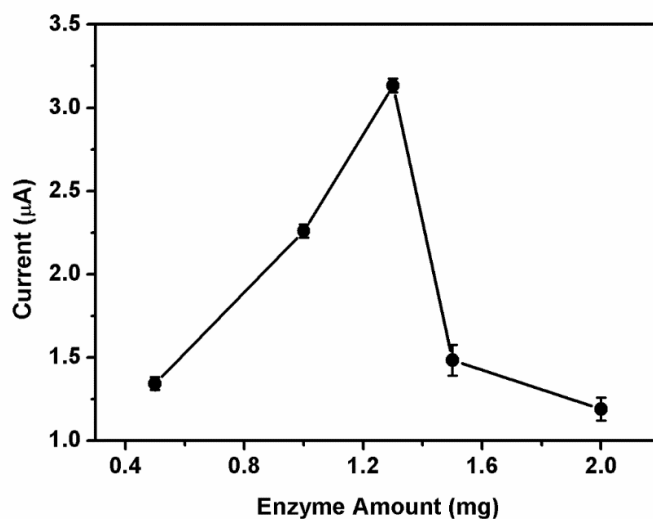


**Figure 2.6.** The effect of loaded enzyme amount on biosensor response (in 50.0 mM PBS, pH 7.0, 25°C). Error bars show the standard deviation (SD) of three measurements.

Finally, the optimum pH value for the system was investigated since enzyme molecules are strongly affected by pH changes which is mainly because of the changes in enzyme conformation at different pH values. Herein, the pH effect was investigated using 50 mM buffer solutions in a pH range of 4.0-9.0 (sodium acetate buffer at pH 4.0-5.5, sodium phosphate buffer at pH 6.0-7.5, tris buffer at pH 8.0-9.0, 25°C). When the responses of the biosensor in these pH values were compared, the highest signal corresponding to the optimum enzyme activity was obtained with pH 7.0 (Figure 2.7).

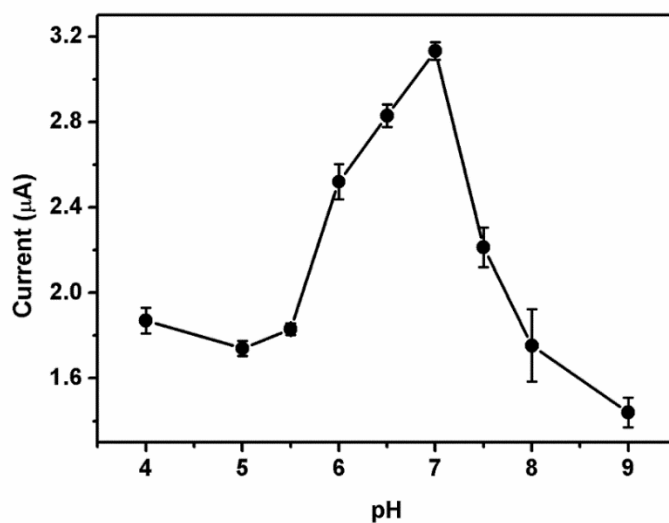


**Figure 2.7.** The effect of pH on biosensor response (in 50 mM sodium acetate buffer at pH 4.0; 5.0; 5.5, 50 mM PBS at pH 6.0; 6.5;7.0;7.5 and 50 mM Tris buffer at pH 8.0 and 9.0, 25°C). Error bars show the standard deviation (SD) of three measurements.

#### 2.2.1.2. Determination of the Best Combination

In order to achieve the best combination for an outstanding biosensor performance, the effects of PFLA, MWCNTs, ZnPc and their different combinations were investigated. Different combinations; pristine PFLA, pristine MWCNTs, pristine ZnPc, MWCNTs/ZnPc, PFLA/MWCNTs and PFLA/MWCNTs/ZnPc were prepared as immobilization matrices using the optimized parameters for the materials and their corresponding signals were compared (Figure 2.8). MWCNTs, which are well known suitable charge transfer reagents, enhance the charge transfer ability and increase the electroactive surface area of the electrodes which results in improved biosensor performance. ZnPc complex also enhances the biosensor performance due to its high chemical stability, redox activity and semi-conducting properties. Moreover, since CPs have the ability to mimic the natural environment for biomolecules, they are improving materials in the biosensor construction. However, when these components were considered separately, prepared electrode surfaces may not be sufficient enough for the proper binding of biomolecules. Also, three-dimensional structure of the enzyme molecules may not be protected causing a decrease in the signal and lifetime

of the biosensor. Furthermore, due to the weak enzyme immobilization, lower stability and sensitivity of the biosensor may show up. Hence, the combination of these three electrode modifier materials resulted in enhanced biosensor performance when compared to the individual use of MWCNT, ZnPc or PFLA species.

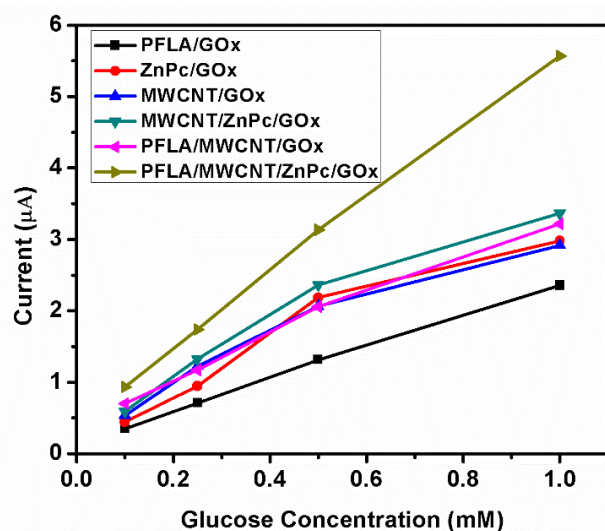


**Figure 2.8.** The effect of different surface modifications on performance of glucose biosensors (in 50.0 mM PBS, pH 7.0, 25°C). Error bars show the standard deviation (SD) of three measurements.

## 2.2.2. Characterizations

### 2.2.2.1. Analytical and Kinetic Characterizations

After determining the optimum conditions for the fabricated biosensor, a calibration curve for glucose was plotted having a linear response range between 0.025-1.0 mM glucose in 50 mM PBS pH 7.0 as given with the equation;  $y = 5.312x + 0.311$  with  $R^2 = 0.997$  (Figure 2.9). At higher glucose concentrations than 1.0 mM, substrate saturation was observed. The LOD and sensitivity values were calculated as 0.018 mM and  $82.18 \mu\text{AmM}^{-1}\text{cm}^{-2}$ , respectively.

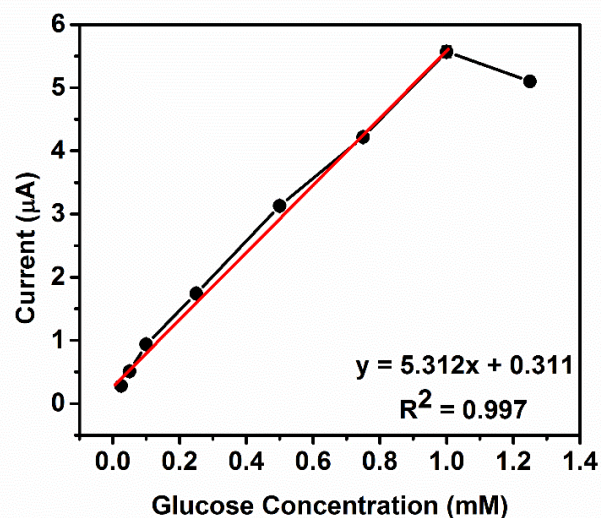


**Figure 2.9.** Calibration curve for glucose (in 50 mM PBS, pH 7.0, 25°C). Error bars show standard deviation (SD) of three measurements.

Moreover, in order to investigate the repeatability of the proposed biosensor, 10 consecutive measurements were successfully recorded for 0.5 mM glucose solution. The SD and RSD values for these measurements were calculated as  $\pm 0.06$  and 3.09%, respectively. The lifetime of the biosensor was also tested by taking amperometric measurements for 30 days with regular time intervals. Only 5% of activity loss was observed at the end of this time proving the reusability of the proposed practical sensing system.

The selectivity of the system was also confirmed since biosensors should detect only the amounts of their target analytes within given samples. The main purpose of glucose biosensors is to detect glucose amounts in blood samples and since there are various biological molecules in the blood, the biosensor should give response to only glucose in order to perform successful analysis with different samples. For this reason, 0.5 mM urea and ascorbic acid solutions were prepared and the effect of these interfering substances was investigated. Instead of glucose, these species were injected to the reaction medium during amperometric measurements and the biosensor response for these substances were recorded. The proposed biosensor did not give any significant

response for these species proving that the system is specific only to its target analyte without possessing any interference effect. (Figure 2.10)

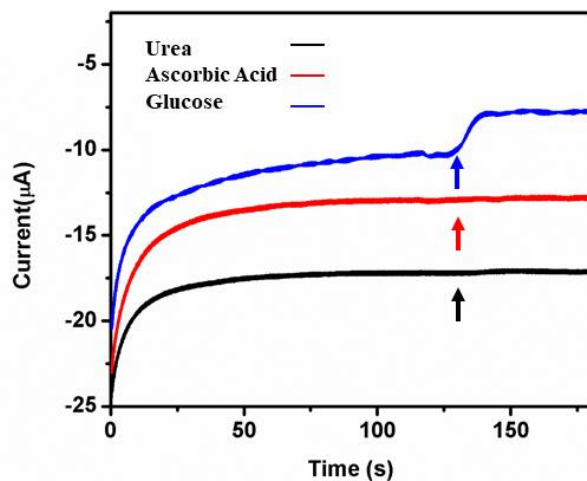


**Figure 2.10.** Biosensor responses to glucose and interfering substances (in 50 mM PBS, pH 7.0, 25 °C).

Furthermore, the kinetic parameters of the proposed biosensor were determined using Michaelis-Menten enzyme kinetics model via Lineweaver-Burk plot. From the equation of this plot,  $K_M^{app}$  and  $I_{max}$  values were calculated as 0.53 mM and 6.12  $\mu A$ , respectively. When these results were compared with the other glucose biosensors in literature,  $K_M^{app}$  value was found to be superior. Chen et al. proposed a biosensor utilizing a pyrolytic graphite electrode modified with nanoscaled cobalt phthalocyanine-glucose oxidase biocomposite. The  $K_M^{app}$  of this biosensor was found as 12.4 mM [84]. Nyokong and co-workers prepared CoPc-CoTPP complexes and Nafion based glucose biosensor having the  $K_M^{app}$  value of 14.91 mM [85]. In another study, a biosensor having an electrode modification of PdNPs-electrochemically reduced graphene oxide possessed the  $K_M^{app}$  value of 5.44 mM [86]. Moreover, Adronov et al. designed a biosensor by entrapping glucose oxidase within the poly[3-(3-N,N-diethylaminopropoxy)thiophene] and single-walled carbon nanotubes films and they obtained the  $K_M^{app}$  value of 3.4 mM [87].

In addition to these enhanced kinetic parameters, the constructed biosensor showed better analytical characteristics with low LOD and high sensitivity values than some other electrochemical glucose biosensor studies in the literature as can be seen in Table 2.1.

**Table 2.1.** Comparison of glucose biosensors in the literature.

<b>Matrices on the electrodes</b>	<b>LOD (mM)</b>	<b>Sensitivity (<math>\mu\text{AmM}^{-1}\text{cm}^{-2}</math>)</b>	<b><math>K_M^{\text{app}}</math> (mM)</b>	<b>Ref</b>
<b>Poly/MWCNT/Zn(II)Pc/GOx</b>	<b>0.018</b>	<b>82.18</b>	<b>0.53</b>	<b>This work</b>
<b>GOD/Nafion/(LbL)<sub>3.5</sub>/ABS</b>	0.05	17.5	NR	[88]
<b>PDDA/PSS/{PDDA- MWCNTs/GOx}<sub>5</sub></b>	0.058	5.6	NR	[89]
<b>graphene-AuNPs-GOD</b>	35	NR	4.73	[90]
<b>Poly(adamantanepyrrole)/SWCNT/<math>\beta</math> -cyclodextrin/GOx</b>	NR	31.02	5	[91]
<b>Au/MPTS-solgel/Au NPs/cysteamine/GOx</b>	0.023	8.3	NR	[92]

NR: Not reported

These improved properties can be attributed to the combination of the CP/MWCNTs/ZnPc providing a great support material for biomolecule immobilization. Herein, PFLA structure enhanced the stability of the system which becomes a durable biosensor as a result of the interactions between the alkyl chains on the polymer backbone and the enzyme molecule since the biomolecule have both hydrophobic and hydrophilic parts in its structure. The  $\pi$ - $\pi$  interactions between the enzyme and polymer also resulted in strong and stable interactions. By this way, no dialysis membrane is required in order to entrap the enzyme molecule. MWCNTs improved the total performance of the sensing system by enhancing the charge transfer

rate and the electroactive surface area. ZnPc structure also increased the biosensor responses due to its high redox activity, chemical stability, semi-conducting properties and biocompatibility. As a result, the combination of this three materials possessed complementary properties due to synergistic effects and thus increase the total performance of the sensing device.

#### **2.2.2.2. Surface Characterizations**

From the peak currents of the corresponding cyclic voltammograms (Figure 2.11), the electroactive surface areas for pristine PFLA, PFLA/MWCNT, PFLA/MWCNT/ZnPc and PFLA/MWCNT/ZnPc/GOx modified electrodes were calculated as 0.038 cm<sup>2</sup>, 0.052 cm<sup>2</sup>, 0.061 cm<sup>2</sup> and 0.046 cm<sup>2</sup>, respectively. The comparable lower electroactive surface area of pristine PFLA than the other electrodes was because of the formation of an additional layer onto the graphite electrode by PFLA coating which passivates the electrode surface. Incorporation of MWCNT and ZnPc resulted in increase in effective surface coverage confirmed by the enhancement of the peak currents which demonstrated the promotion of the electron transfer rate and the redox reaction of the probe by these materials. Also, strong  $\pi$ - $\pi$  interaction between the ZnPc molecule and MWCNT/PFLA combination was a strong evidence of the highest electroactive surface area of PFLA/MWCNT/ZnPc. Furthermore, enzyme immobilization caused the decrease in the peak current and therefore in the effective surface area which was because of the insulating character of the biomolecules.

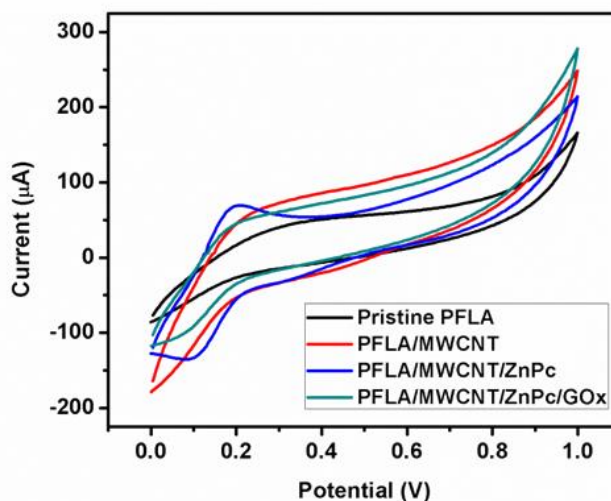


**Figure 2.11.** Cyclic voltammograms resulting from pristine PFLA, PFLA/MWCNT, PFLA/MWCNT/ZnPc and PFLA/MWCNT/ZnPc/GOx in 5.0 mM  $\text{Fe}(\text{CN})_6^{3-/4-}$  containing 0.1 M KCl.

SEM technique was used for surface morphology characterization of surfaces. In Figure 2.12, SEM images represent pristine PFLA, PFLA/MWCNTs/ZnPc and PFLA/MWCNTs/ZnPc/GOx modified electrode surfaces, respectively. Each surface change proved the proper surface modification. PFLA deposition resulted in a fully covered homogenous film. Incorporation of MWCNT and ZnPc complex to PFLA modified electrode surface led to a successful distribution of ZnPc complex molecules with the help of uniform MWCNT distribution. The layered structures were rougher than the morphology of pristine PFLA coating which indicates the successful PFLA/MWCNT/ZnPc combination. A significant morphology change was observed after the GOx immobilization. Homogeneous coating of the enzyme proved that the proposed electrode modification serves as a great host-guest platform for biomolecule deposition.

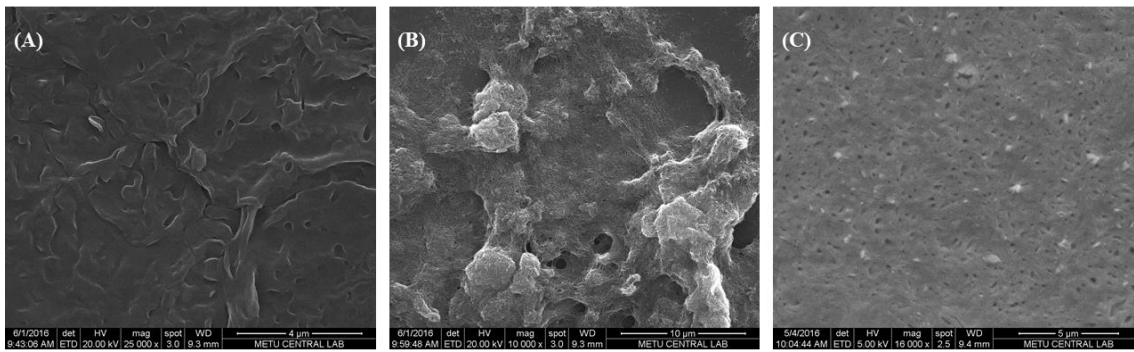


**Figure 2.12.** SEM images of (A) pristine PFLA; (B) PFLA/MWCNT/ZnPc; (C) PFLA/MWCNT/ZnPc/GOx under optimized conditions.

### 2.2.3. Application of the Biosensor

The feasibility of the proposed sensing system for real sample analyses was investigated by testing the biosensor with different commercial beverages. During amperometric measurements, the beverage samples were injected into the reaction medium and the glucose contents of these samples were calculated using the calibration curve. As given in Table 2.2, results were very close to the product label values demonstrating that the constructed biosensor is applicable for practical sample testing with reliable accuracy and precision.

**Table 2.2.** Results of glucose analysis in beverages.

Sample	Glucose Content (mM)		Relative Error (%)
	Product Label	PFLA/MWCNTs/ZnPc/GOx	
S® Milk	0.25	0.247	-1.20
L® Ice tea	0.37	0.350	-5.41
C® Coke	0.62	0.598	-3.55

## CHAPTER 3

### PFLA/PAMAM/MWCNTs/GO<sub>x</sub> BIOSENSOR

#### 3.1. Experimental

##### 3.1.1. Materials and Methods

Glucose oxidase (GO<sub>x</sub>, β-D-glucose: oxygen 1-oxidoreductase EC 1.1.3.4, 17,300 units/g solid) from *Aspergillus niger* and D-glucose were obtained from Sigma (St. Louis, USA). Poly (amidoamine) (PAMAM)-25% C12 dendrimer, generation 2.0, 20 wt% solution in methanol, PAMAM-25% C12 dendrimer, generation 4.0, 10 wt% solution in methanol, multi walled carbon nanotubes (MWCNTs), glutaraldehyde (GA) and chloroform were purchased from Sigma–Aldrich Co., LCC. (St. Louis, USA). The polymer, poly[9,9-di-(2-ethylhexyl)-fluorenyl-2,7-diyl] end capped with N,N-bis (4-methylphenyl)-4- aniline (PFLA), was obtained from American Dye Source, Inc. (Quebec, Canada). Dimethylformamide (DMF) was purchased from Carlo Erba Reagents SAS (Reuil, France). For enzyme immobilization, 50 mM pH 7.0 phosphate buffer solution (PBS) was prepared from 0.025 M Na<sub>2</sub>HPO<sub>4</sub> (Fisher Scientific Company) and 0.025 M NaH<sub>2</sub>PO<sub>4</sub> (Fisher Scientific Company). As the substrate, glucose solution (0.1 M) was prepared by dissolving 0.18 g of D-glucose in 10 mL pH 7.0 PBS.

All the amperometric measurements and cyclic voltammetry studies were performed using EmStat3 potentiostat (PalmSens, Houten, The Netherlands). Three electrode system consisting of a graphite rod working electrode (Ringsdorff Werke GmbH, Bonn, Germany, typeRW001, 3.05 mm diameter and 13% porosity), Pt wire counter electrode (Metrohm, Switzerland) and Ag wire reference electrode was used for all electrochemical studies. Scanning electron microscope (SEM) (JEOL JSM-6400 model) was used for the surface modification characterization of the fabricated biosensor. All measurements were conducted at ambient conditions.

### 3.1.2. Preparation of the Biosensor

Before surface modification, spectroscopic grade graphite rods were polished on emery paper and washed with distilled water. 20  $\mu\text{L}$  aliquots of CP solution prepared by dissolving 2.0 mg PFLA in 2.0 mL chloroform, were deposited on a cleaned graphite electrode surface. 0.75 mg MWCNT were dispersed in 10 mL DMF by ultrasonication for 15 min to obtain a black suspension. Then, 20  $\mu\text{L}$  aliquots of this suspension were cast on CP modified electrode surface. PAMAM solution was prepared as 0.4 mM by diluting with methanol and when the electrode was dried, 10  $\mu\text{L}$  aliquots of PAMAM solution were cast on the surface of the electrode. For the enzyme immobilization, certain amount of GOx was dissolved in 10.0  $\mu\text{L}$  of PBS (50 mM, pH 7.0) and this solution was immobilized on the dried electrode surface followed by the addition of 6.0  $\mu\text{L}$  of GA (1% in 50 mM PBS pH 7.0) to the electrode surface. The prepared electrode was left to dry for 2 h at ambient conditions, rinsed with distilled water to remove the unbound molecules and impurities. Figure 3.1 illustrates schematic representation of the procedure for the construction of the proposed biosensor.

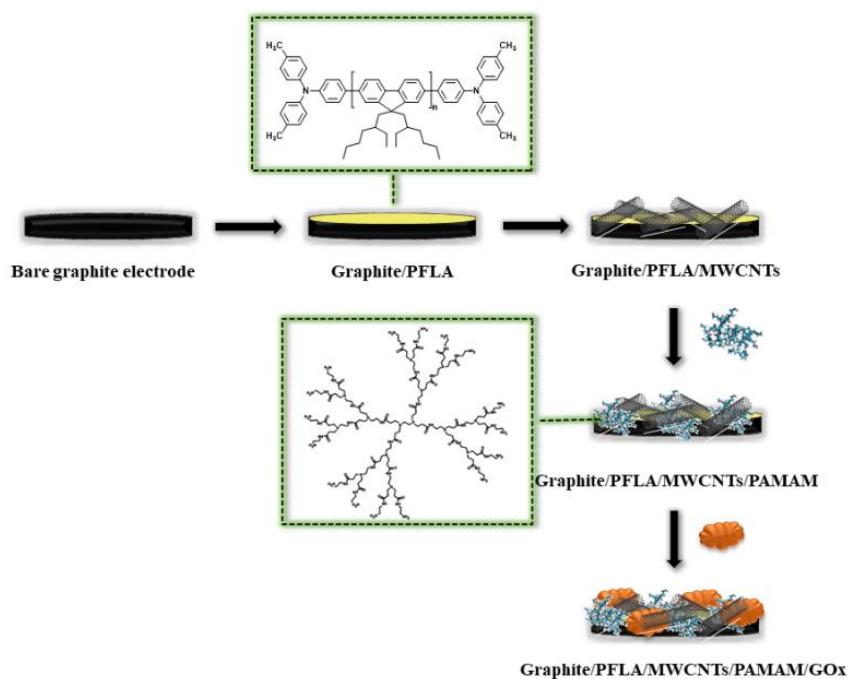


**Figure 3.1.** Schematic representation of PFLA/MWCNTs/PAMAM/GOx Biosensor

### **3.1.3. Amperometric Measurements**

All amperometric studies were performed in a reaction cell filled with 10 mL pH 7.0 PBS solution by applying -0.7 V constant potential at ambient conditions under mild stirring. As a result of the enzymatic reaction between GOx and the substrate, the decrease in the oxygen level associated with substrate concentration was monitored at -0.7 V potential. The buffer solution was refreshed and the electrodes were washed with distilled water, then kept in buffer solutions for a while after each measurement. In all amperometric studies, each measurement was carried out three times repetitively and the data were given as the average of these measurements and standard deviations were recorded as  $\pm$ SD.

### **3.1.4. Optimization of Biosensor Performance**

All the parameters affecting the biosensor performance in the construction were optimized in order to obtain a stable and reproducible biosensor response. In this study, the effects of different amounts of CP, MWCNTs and PAMAM as well as the enzyme concentration and pH values on the current signal were investigated. Different electrodes were prepared by changing only the amount of the parameter to be optimized. The one with the highest signal was chosen as the optimum value and used for the biosensor construction at further steps.

### **3.1.5. Characterizations**

#### **3.1.5.1. Analytical and Kinetic Characterizations**

After determining the optimum conditions for the proposed biosensor, a calibration curve for glucose was plotted. The LOD and sensitivity values were calculated by setting the intercept of the linear range of the calibration curve to zero using  $S/N = 3$  criterion. For the repeatability testing, 20 consecutive measurements were done for 0.5 mM glucose solution and SD and RSD values were calculated for these measurements. Moreover, the lifetime of the biosensor was measured by taking amperometric

measurements with regular time intervals for 30 days. Percent activity loss value was calculated at the end of this time.

For the kinetic characterization studies, Michaelis-Menten enzyme kinetics model was used. From Lineweaver-Burk plot ( $1/I$  vs  $1/[S]$ ),  $I_{\max}$  and  $K_M^{\text{app}}$  values were calculated.

### **3.1.5.2. Surface Characterizations**

CV studies were performed in order to characterize the effective electroactive surface area for each modification. Experiments were conducted in a reaction cell containing 5.0 mM  $\text{Fe}(\text{CN})_6^{3-/4-}$ , 0.1 M KCl and 50.0 mM PBS pH 7.0 by applying the potential between 0 and 1.0 V with a scan rate of  $100 \text{ mV s}^{-1}$ . Determination of electroactive surface areas for each modification was performed using Randles-Sevcik equation.

SEM technique was also used for surface morphology characterization for different surface modifications. Images of pristine PFLA, PFLA/MWCNTs, PFLA/MWCNTs/PAMAM and PFLA/MWCNTs/PAMAM/GOx modified electrode surfaces were analyzed.

### **3.1.6. Sample Application**

The fabricated biosensor was tested on different commercially available beverage samples in order to prove the applicability of the system. The samples were directly injected into the reaction medium and their corresponding current signal were recorded. From the equation of the calibration curve, the glucose contents of these samples were determined and relative error values were calculated.

## **3.2. Results and Discussion**

### **3.2.1. Optimization Studies**

#### **3.2.1.1. Optimization of the Biosensor Parameters**

First of all, in order to obtain a proper orientation and effective binding of the enzyme on CP surface, optimum CP amount was investigated by dissolving 1.0, 1.5, 2.0, 2.5 and 3.0 mg of PFLA in 2.0 mL chloroform. 20  $\mu\text{L}$  aliquots of these solutions were cast on graphite electrode surfaces for different biosensors and their corresponding signals

were compared by keeping all the other parameters constant. 2.0 mg PFLA resulted in the highest biosensor response (Figure 3.2).

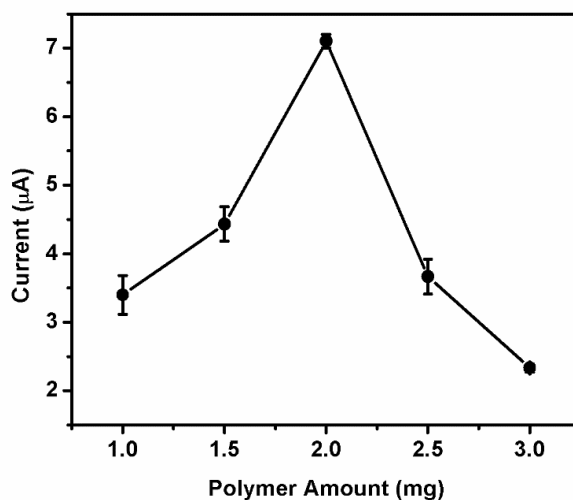


**Figure 3.2.** The effect of polymer amount on biosensor response (in 50.0 mM PBS, pH 7.0, 25°C). Error bars show the standard deviation (SD) of three measurements.

Then, the effect of different MWCNTs amount on the biosensor performance was investigated since higher amounts of MWCNTs resulted in lower biosensor responses due to diffusional constraints; whereas lower MWCNTs amounts affected the biosensor responses since it causes improper accommodation of enzyme molecules onto the electrode surface. In order to optimize the MWCNTs amount, different biosensors were prepared with 0.25, 0.50, 0.75, 1.00 and 1.50 mg of MWCNTs. According to the compared results, the highest response was obtained with 0.75 mg MWCNTs (Figure 3.3).

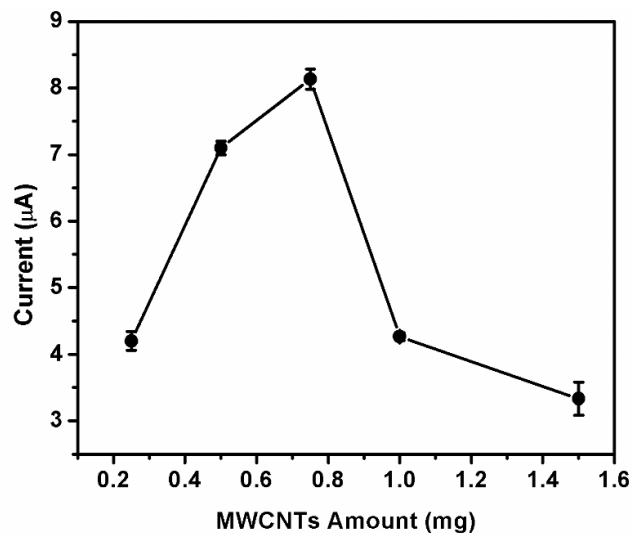


**Figure 3.3.** The effect of MWCNTs amount on biosensor response (in 50.0 mM PBS, pH 7.0, 25°C). Error bars show the standard deviation (SD) of three measurements.

Furthermore, the concentration of PAMAM was optimized using different PAMAM solutions having 0.2, 0.3, 0.4, 0.5 and 0.6 mM concentrations in biosensor fabrication. When the recorded signals were compared, biosensor response increased to a maximum value with 0.4 mM for PAMAM. After that point, a significant decrease in the signal was observed which was because higher amounts of dendrimers could prevent the approach of substrate to the electrode surface. Thus, the saturation of the dendrimer structure resulted in lower electrocatalytic activity (Figure 3.4).

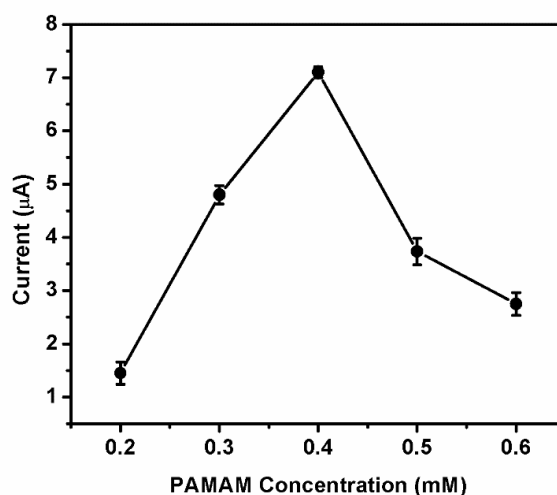


**Figure 3.4.** The effect of PAMAM concentration on biosensor response (in 50.0 mM PBS, pH 7.0, 25°C). Error bars show the standard deviation (SD) of three measurements.

Moreover, enzyme amount was optimized in order to reach to the loading capacity of the immobilization matrix. To determine the best enzyme amount for the immobilization matrix, five different electrodes with 1.0 mg (17.3 U), 2.0 mg (34.6 U), 2.6 (45.0 U), 3.0 mg (51.9 U), 4.0 mg (69.2 U) GOx were prepared and the corresponding responses were compared. 2.6 mg GOx resulted in the highest biosensor signal (Figure 3.5).

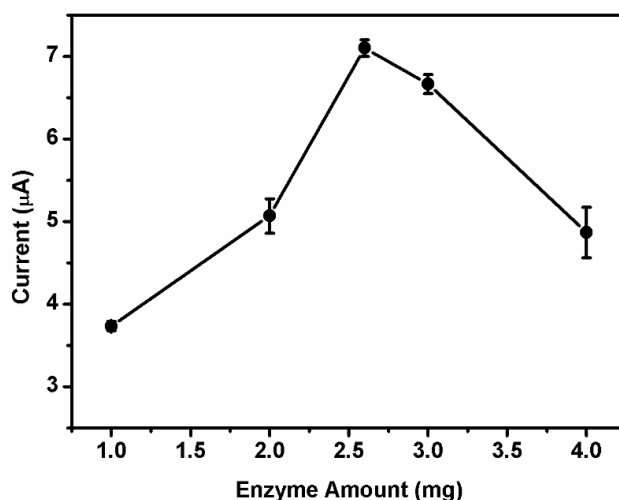


**Figure 3.5.** Effect of enzyme amount on biosensor response (in 50.0 mM PBS, pH 7.0, 25°C). Error bars show the standard deviation (SD) of three measurements.

Finally, the optimum pH value was investigated to obtain the highest enzyme activity since pH changes strongly affect the orientation and stability of enzyme molecules. The pH effect was investigated using 50 mM buffer solutions in a pH range of 5.0-9.0 (sodium acetate buffer at pH 4.0-5.5, sodium phosphate buffer at pH 6.0-7.5, tris buffer at pH 8.0-9.0, 25 °C). When the biosensor responses in different buffer solutions were compared, the highest enzyme activity was obtained with pH 7.0 (Figure 3.6).

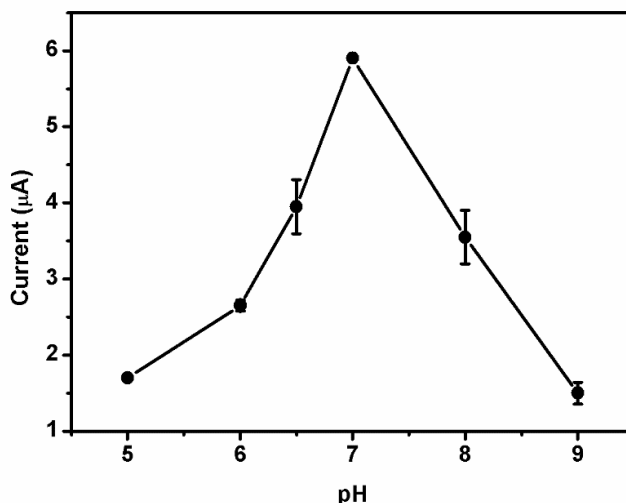


**Figure 3.6.** Effect of pH (in 50 mM sodium acetate buffer at pH 4.0; 5.0; 5.5, 50 mM PBS at pH 6.0; 6.5; 7.0; 7.5 and 50 mM tris buffer at pH 8.0 and 9.0) on biosensor response. Error bars show the standard deviation (SD) of three measurements.

### 3.2.1.2. Determination of the Best Combination

In order to improve the immobilization and enhance the interaction between the polymer and enzyme molecules, MWCNTs were incorporated onto CP modified electrode surface. After that, the biosensor was further functionalized with PAMAM dendrimer to get more reactive regions for the attachment of GOx to obtain more sensitive glucose detection. For this purpose, two different biosensors were prepared with PAMAM G2 and PAMAM G4 structures separately (Figure 3.7). When the performances of these two biosensors were compared, the biosensor prepared with PAMAM G2 gave higher and more stable responses since as PAMAM dendrimer size increases, resistivity in flexibility increased and the detection sensitivity was limited. Moreover, Demirci et al. pointed out that  $K_M^{app}$  value is lower in the case of PAMAM

G2 modification compared to the PAMAM G4 modification [93]. This also proves that the enzyme activity is higher in the more flexible PAMAM G2 environment. Furthermore, Miura et al. compared the amount of adsorbed protein onto different PAMAM generations [94]. They showed that as dendrimer size increases, adsorption of protein molecules decreases showing that dendrimer surface with a high generation results in higher bio-inertness. Therefore, in this system, further modification of CP/MWCNTs combination was performed with the utilization of PAMAM G2 dendrimer. As a result, the best immobilization platform for the enzyme was designed as CP/MWCNTs/PAMAM G2 dendrimer.

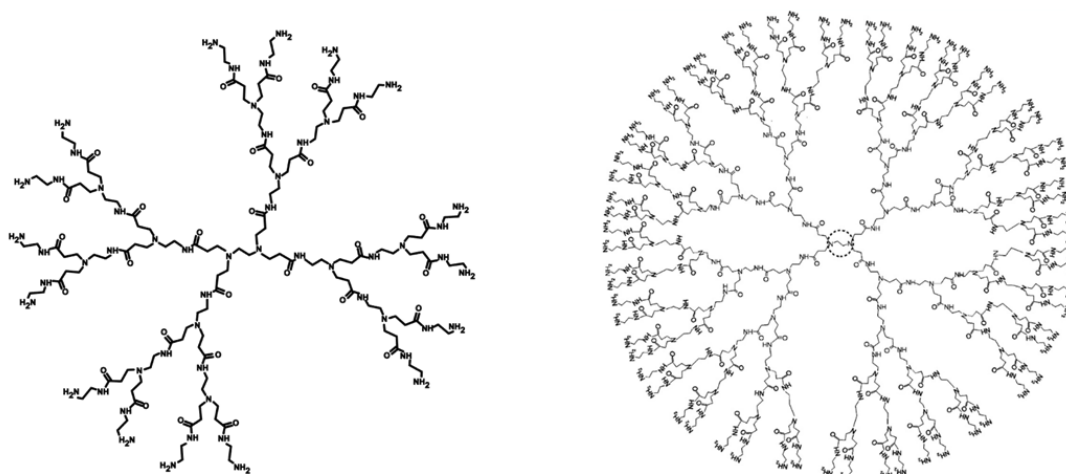


**Figure 3.7.** Structures of PAMAM G2 and PAMAM G4

### 3.2.2. Characterizations

#### 3.2.2.1. Surface Characterizations

From the peak currents of cyclic voltammograms, the electroactive surface areas for different combinations; bare graphite, PFLA/MWCNTs, PFLA/MWCNTs/PAMAM and PFLA/MWCNTs/PAMAM/GOx, were calculated as 0.64 cm<sup>2</sup>, 0.87 cm<sup>2</sup>, 1.28 cm<sup>2</sup> and 0.63 cm<sup>2</sup>, respectively (Figure 3.8). A well-defined oxidation peak for the bare graphite electrode was observed proving the proper working electrode property of the graphite rod. When the MWCNTs modification to the PFLA coated electrode was performed, the resulted enhancement of the peak current demonstrated that MWCNTs

facilitate the charge transfer rate and the redox reaction. A further increase in the peak current in the case of PAMAM modification is attributed to the electrostatic adsorption affinity of the positively charged PAMAM molecules to the negatively charged  $\text{Fe}(\text{CN})_6^{3-/4-}$  species. After GOx immobilization, the decrease in the peak current due to the insulating character of the biomolecules confirmed the effective attachment of the enzyme on the electrode.

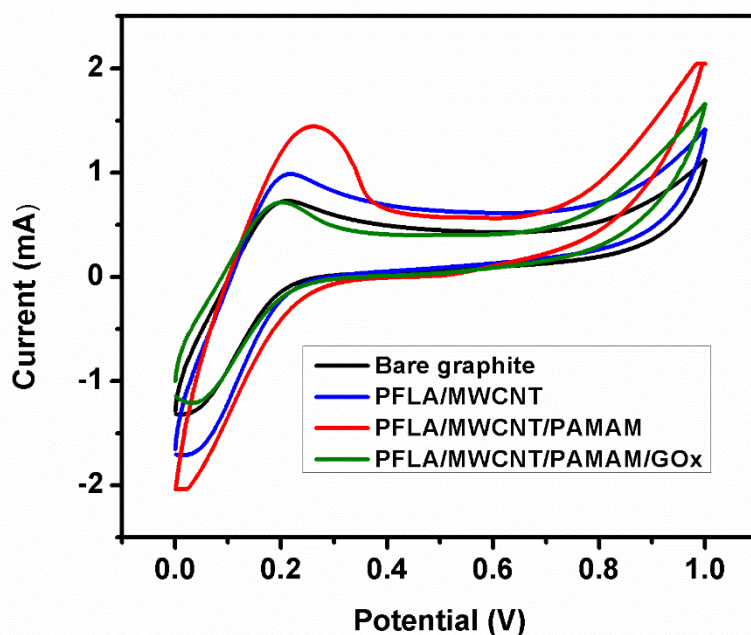


**Figure 3.8.** Cyclic voltammograms resulting from a bare graphite, PFLA/MWCNT, PFLA/MWCNT/PAMAM and PFLA/MWCNT/PAMAM/GOx in 5.0 mM  $\text{Fe}(\text{CN})_6^{3-/4-}$  containing 0.1 M KCl.

The effect of different surface modifications was investigated with SEM technique. In Figure 3.9, SEM images represent the electrodes with pristine PFLA, PFLA/MWCNTs, PFLA/MWCNTs/PAMAM and PFLA/MWCNTs/PAMAM/GOx modifications, respectively. Homogenous distribution of PFLA molecules were observed when the electrode was coated with PFLA solution. When MWCNTs were incorporated to CP modified surface, both the structures of PFLA and MWCNTs were observed clearly as a result of proper interaction between the structures. Further modification with PAMAM resulted in rough layered structures proving the successful PFLA/MWCNTs/PAMAM combination. After the GOx immobilization, a significant

morphology change was observed possessing a homogeneous surface coating. This also proved that the designed electrode surface serves as a great host-guest platform for biomolecule deposition.

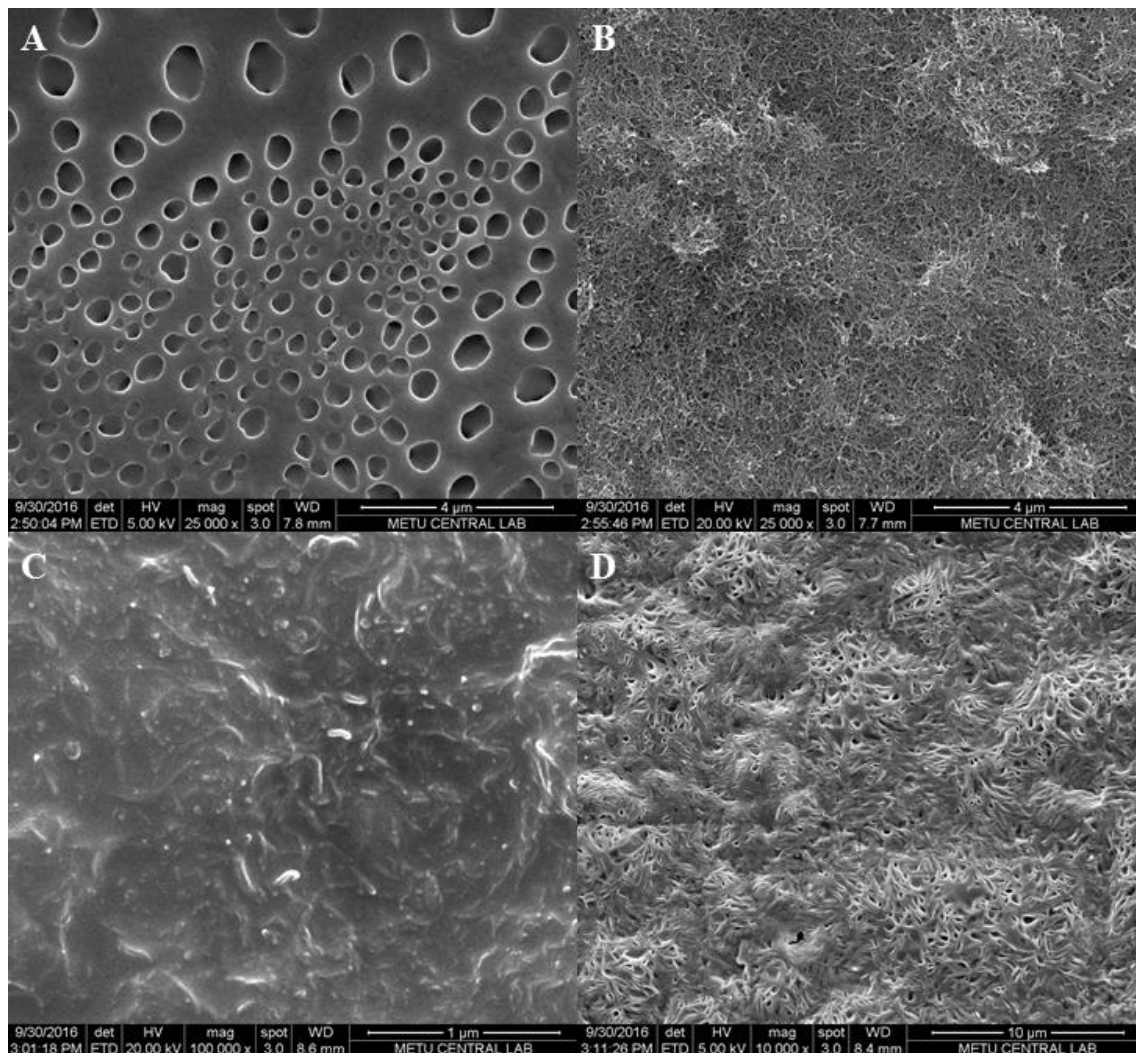


**Figure 3.9.** SEM images of (A) pristine PFLA; (B) PFLA/MWCNT; (C) PFLA/MWCNT/PAMAM (D) PFLA/MWCNT/PAMAM/GO<sub>x</sub> under the optimized conditions.

### 3.2.2.2 Analytical and Kinetic Characterizations

After all the optimum conditions were determined, a calibration curve for glucose was plotted to relate the current to different substrate concentrations (Figure 3.10). A good linearity between 0.05 and 0.75 mM glucose as given with the equation  $y = 14.089x$

+ 0.767 with  $R^2 = 0.996$  was obtained. The LOD and sensitivity values were calculated as 0.014 mM and  $55.41 \mu\text{A mM}^{-1}\text{cm}^{-2}$ , respectively.

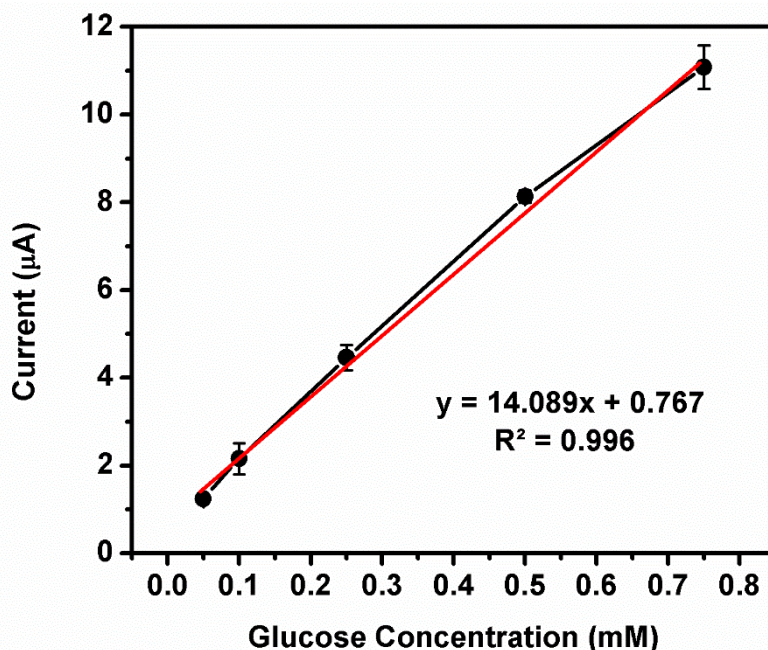


**Figure 3.10.** Calibration curve for glucose (in 50 mM PBS, pH 7.0, 25 °C). Error bars show standard deviation of three measurements.

In order to prove the repeatability of the biosensor, 20 consecutive measurements were successfully performed with the SD and RSD values of  $\pm 0.16$  and 2.90%, respectively. The lifetime of the biosensor was also tested by taking amperometric measurements with regular time intervals for 30 days. At the end of this time, 5.9% of activity loss was observed which confirms the reusability of the fabricated biosensor.

In order to test the selectivity of the fabricated glucose biosensor, the effect of interfering substances was investigated by testing the biosensor with 0.5 mM urea and ascorbic acid solutions since these compounds can easily be oxidized at bare electrodes. When these species were injected to the reaction medium during amperometric measurements, the biosensor did not give any significant response to these species showing that there is no interference at -0.7 V potential under the optimized conditions (Figure 3.11).

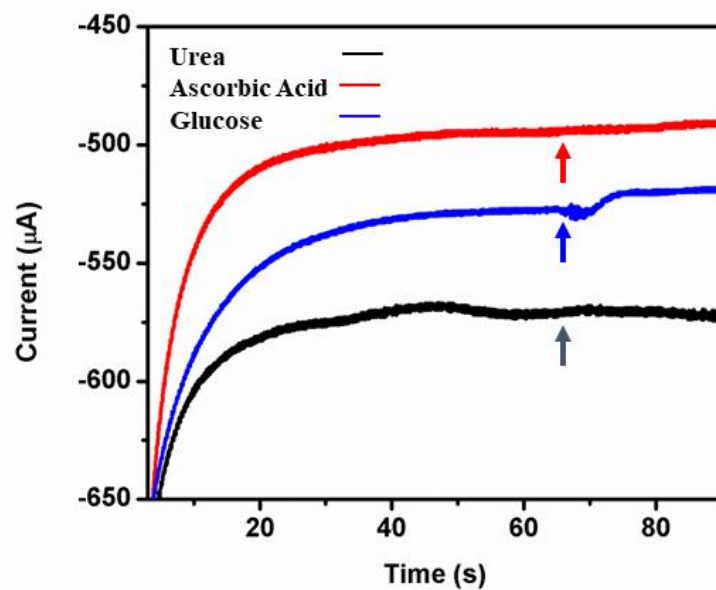


**Figure 3.11.** Biosensor responses to glucose and interfering substances (in 50 mM PBS, pH 7.0, 25 °C).

Moreover, the kinetic parameters of the proposed biosensor were determined from the Lineweaver-Burk plot.  $K_M^{app}$  and  $I_{max}$  values were calculated as 0.66 mM and 17.39  $\mu\text{A}$ , respectively. When these parameters were compared with the literature,  $K_M^{app}$  value was found to be superior and the biosensor possessed enhanced analytical properties with low LOD and high sensitivity values. Liu et al. proposed a glucose biosensor based on water-dispersible chitosan-functionalized graphene (CG) further modified with  $\text{Fe}_3\text{O}_4$ . The biosensor have a sensitivity value of  $5.658 \mu\text{AmM}^{-1}\text{cm}^{-2}$  with a detection limit of 16  $\mu\text{M}$  [95]. In another study, Singh et al. developed a biosensor via immobilization of GOx on sulfonated graphene/AuNPs/chitosan nanocomposite which possess the  $K_M^{app}$  value of 1.96 mM and sensitivity value of  $6.51 \mu\text{AmM}^{-1}\text{cm}^{-2}$  [96]. In another biosensor fabricated by Araque et al., GOx immobilization on a glassy carbon electrode coated with a hybrid nanomaterial of anchored (3-glycidyloxypropyl)trimethoxysilane at the surface of graphene oxide, further cross-linked with PAMAM G4 dendrimer and modified with platinum nanoparticles, resulted in the  $K_M^{app}$  value of 6.9 mM and sensitivity value of  $24.6 \mu\text{AmM}^{-1}\text{cm}^{-2}$  [97]. Fernandes and co-workers presented a biosensor with 5.71 mM

$K_M^{app}$  in which streptokinase, GOx and phosphorylcholine were immobilized onto polyglycerol dendrimer which was then entrapped in polyaniline nanotubes [98]. The enhanced characteristics of the fabricated biosensor were further compared with some other literature examples in Table 3.1. The enhancing effect of MWCNTs-PAMAM combination is well studied in the literature. In this work, the improved performance can be attributed to the incorporation of the CP to MWCNTs/PAMAM combination which provides an enhanced immobilization matrix for the enzyme.

**Table 3.1.** Comparison of glucose biosensors in the literature.

<b>Matrices on the electrodes</b>	<b>LOD (mM)</b>	<b>Sensitivity (<math>\mu\text{AmM}^{-1}\text{cm}^{-2}</math>)</b>	<b><math>K_M^{app}</math> (mM)</b>	<b>Ref</b>
<b>Poly/MWCNT/PAMAM/GOx</b>	<b>0.014</b>	<b>55.41</b>	<b>0.66</b>	<b>This work</b>
<b>GOD/CNTs/CS/GC</b>	NR	7.36	8.2	[99]
<b>MWCNT/GO/GOx</b>	0.028	3.37	NR	[100]
<b>Au/MPA/Fc-PAMAM-G2</b>	0.33	25.2	22.92	[101]
<b>PAMAM G4-HYM/GOx</b>	NR	0.028	5.2	[102]
<b>GOD/graphitic nanocage modified GCE</b>	8	13.3	NR	[103]

NR: Not Reported

### 3.2.3. Application of the Biosensor

The proposed biosensor was tested on different commercial beverages in order to prove the feasibility of the sensing system. The beverage samples were injected into the reaction medium without any pretreatment and their corresponding signals were recorded. The glucose contents of the samples were calculated by inserting the biosensor signals into the equation of the calibration curve and the results were compared with the product label values. As given in Table 3.2, results are very close to the product label values proving the applicability of the fabricated biosensor for real time analyses with reliable accuracy and precision.

**Table 3.2.** Results of glucose analysis in beverages.

Sample	Glucose Content		Relative Error (%)
	(mM)		
	Product Label	PFLA/MWCNTs/PAMAM/GOx	
S® Milk	0.25	0.239	4.40
U®Lemon Soda	0.47	0.450	4.26
C® Coke	0.62	0.610	1.61



## CHAPTER 4

### CONCLUSION

In this thesis, two different biosensors with different matrices were constructed for the purpose of glucose detection. Glucose oxidase was used as a model enzyme for fabrication of these two biosensing systems. A functional conjugated polymer PFLA together with multi-walled carbon nanotubes was used as an immobilization matrix for both biosensors. Utilization of the conjugated polymer improved the feature of the enzyme immobilization since the presence of alkyl chains on the polymer backbone provided strong interaction with the hydrophobic parts of the enzyme molecule and the  $\pi$ - $\pi$  stacking between the aromatic residues of the enzyme and polymer enhanced the physical interactions leading to a stable biosensor platform. Modification with multi-walled carbon nanotubes enhanced the charge transfer rate which results in more sensitive and faster biosensor responses by enlarging the electroactive surface areas of the electrodes. The electrode surfaces were further modified with different macrostructures in order to investigate their effects on biosensor performance.

In the first study, water soluble zinc phthalocyanine molecule was used as the macrostructure modifier owing to its promising electronic properties with rich redox chemistry and stability. To the best of our knowledge, a sensor design which combines conjugated polymer/MWCNTs/ZnPc was attempted for the first time and this approach resulted in improved biosensor characteristics. Via the combination of these three materials, the biosensor possessed complementary properties due to synergistic effects and enhanced the total performance of the sensing device. PFLA/MWCNTs/ZnPc/GOx biosensor showed a long term stability and good linear response for glucose between 0.025-1.0 mM with a detection limit of 0.018 mM and the sensitivity value of  $82.18 \mu\text{Amm}^{-1}\text{cm}^{-2}$ . The proposed sensing system also presented superior kinetic parameters with the  $K_M^{\text{app}}$  value of 0.53 mM. Moreover, scanning electron microscopy and cyclic voltammetry techniques were used to

investigate the surface modifications. Finally, the fabricated biosensor was successfully tested on beverages for glucose detection. Satisfactory results were obtained indicating that the proposed sensing system is an important tool for real time analyses for glucose determination.

*This study was published in International Journal of Biological Macromolecules in 2017 [104].*

In the second study, amperometric biosensing performance of a novel platform utilizing a conjugated polymer, multi-walled carbon nanotubes and poly(amidoamine) dendrimer was investigated. The highly-branched dendritic macromolecule was utilized since it improves the biomolecule attachment due to the presence of a number of terminal amino groups in its structure. The analytical and kinetic parameters of the constructed biosensor were investigated and the biosensor presented a linear response for glucose between 0.05 and 0.75 mM with a detection limit of 0.014 mM.  $K_M^{app}$  and sensitivity values were calculated as 0.66 mM and  $55.41 \mu\text{Amm}^{-1}\text{cm}^{-2}$ , respectively. The improved performance of the study was attributed to the addition of the conjugated polymer to the enhancing effect of MWCNTs-PAMAM combination which is well studied in the literature. To investigate the surface modifications, scanning electron microscopy and cyclic voltammetry techniques were used. Finally, fabricated biosensor was tested on beverages for glucose detection successfully. The obtained satisfactory results indicated that the proposed biosensor is an important tool for real time analyses for glucose determination.

*This study was published in Journal of Electroanalytical Chemistry in 2017 [105].*

## REFERENCES

- [1] S. P. J. Higson, "Enzyme and other biosensors: evolution of a technology," *Eng. Sci. Educ. J.*, vol. 3, no. 1, p. 41, 1994.
- [2] D. M. Fraser, "Glucose biosensors— The sweet smell of success," *Med. Device Technol.*, vol. 5, no. 9, pp. 44–47, 1994.
- [3] D. R. Thévenot, K. Toth, R. A. Durst, and G. S. Wilson, "Electrochemical biosensors: Recommended definitions and classification," *Biosens. Bioelectron.*, vol. 16, no. 1–2, pp. 121–131, 2001.
- [4] L. Clark Jr, "Membrane polarographic electrode system and method with electrochemical compensation," US3539455A, 1970.
- [5] Z. Altintas, *Biosensors and Nanotechnology*. John Wiley & Sons, Inc, 2018.
- [6] M. Gerard, A. Chaubey, and B. D. Malhotra, "Application of conducting polymers to biosensors," *Biosens. Bioelectron.*, vol. 17, no. 5, pp. 345–359, 2002.
- [7] T. Ahuja, I. A. Mir, D. Kumar, and Rajesh, "Biomolecular immobilization on conducting polymers for biosensing applications," *Biomaterials*, vol. 28, no. 5, pp. 791–805, 2007.
- [8] N. Gupta, S. Sharma, I. A. Mir, and D. Kumar, "Advances in sensors based on conducting polymers," *J. Sci. Ind. Res. (India)*, vol. 65, no. 7, pp. 549–557, 2006.
- [9] S. P. MOHANTY and E. KOUGIANOS, "Biosensors: A tutorial review," *IEEE Potentials*, no. April, pp. 35–40, 2006.
- [10] F. Bright, "Optical and Piezoelectric Biosensors," *Anal. Chem.*, vol. 59, no. 19, pp. 1161–1163, 1987.
- [11] A. Chaubey and B. D. Malhotra, "Mediated biosensors," *Biosens. Bioelectron.*, vol. 17, no. 6–7, pp. 441–456, 2002.
- [12] J. Wang, "Electrochemical biosensors: Towards point-of-care cancer diagnostics," *Biosens. Bioelectron.*, vol. 21, pp. 1887–1892, 2006.
- [13] P. D'Orazio, "Biosensors in clinical chemistry," *Clin. Chim. Acta*, vol. 334, no. 1–2, pp. 41–69, 2003.
- [14] D. Grieshaber, R. MacKenzie, J. Vörös, and E. Reimhult, "Electrochemical Biosensors - Sensor Principles and Architectures," *Sensors*, vol. 8, no. 12, pp. 1400–1458, 2008.

- [15] R. M. Ianniello and A. M. Yacynych, "Immobilized enzyme chemically modified electrode as an amperometric sensor," *Anal. Chem.*, vol. 53, no. 13, pp. 2090–2095, 1981.
- [16] J. Wang, *Analytical Electrochemistry*, 3rd ed. Hoboken New Jersey USA: John Wiley & Sons VCH.
- [17] S. R. Mikkelsen and G. A. Rechnitz, "Conductometric Transducers for Enzyme-Based Biosensors," *Anal. Chem.*, vol. 61, no. 15, pp. 1737–1742, 1989.
- [18] N. J. Ronkainen, H. B. Halsall, and W. R. Heineman, "Electrochemical biosensors," *Chem. Soc. Rev.*, vol. 39, no. 5, p. 1747, 2010.
- [19] P. N. Bartlett, Ed., *Bioelectrochemistry Fundamentals, Experimental Techniques and Applications*. West Sussex, England: John Wiley & Sons, 2008.
- [20] S. F. D'Souza, "Immobilization and stabilization of biomaterials for biosensor applications," *Appl. Biochem. Biotechnol. - Part A Enzym. Eng. Biotechnol.*, vol. 96, no. 1–3, pp. 225–238, 2001.
- [21] M. M. F. Choi, "Progress in enzyme-based biosensors using optical transducers," *Microchim. Acta*, vol. 148, no. 3–4, pp. 107–132, 2004.
- [22] A. Dwevedi and A. M. Kayastha, "Enzyme immobilization: A breakthrough in enzyme technology and boon to enzyme based industries," *Proteomics Res. J.*, vol. 3, no. 4, pp. 333–352, 2012.
- [23] Z. Zhao and H. Jiang, "Enzyme-based Electrochemical Biosensors," in *Biosensors*, vol. 6, no. 1, P. A. Serra, Ed. InTech, 2010, pp. 6–9.
- [24] B. G.F., "Immobilization of Enzymes and Cells," in *Methods in Biotechnology*, 1st ed., Bickerstaff G.F., Ed. Humana Press, 1997.
- [25] S. Datta, L. R. Christena, and Y. R. S. Rajaram, "Enzyme immobilization: an overview on techniques and support materials," *Biotechnology*, vol. 3, no. 1, pp. 1–9, 2013.
- [26] A. Sassolas, L. J. Blum, and B. D. Leca-Bouvier, "Immobilization Strategies," *Biotechnol. Adv.*, vol. 30, pp. 489–511, 2012.
- [27] S. Borgmann, G. Hartwich, A. Schulte, and W. Schuhmann, "Amperometric Enzyme Sensors based on Direct and Mediated Electron Transfer," in *Perspectives in Bioanalysis*, vol. 1, no. C, 2005, pp. 599–655.
- [28] W. H. Scouten, J. H. T. Luong, and R. Stephen Brown, "Enzyme or protein immobilization techniques for applications in biosensor design," *Trends Biotechnol.*, vol. 13, no. 5, pp. 178–185, 1995.
- [29] I. Migneault, C. Dartiguenave, M. J. Bertrand, and K. C. Waldron, "Glutaraldehyde: Behavior in aqueous solution, reaction with proteins, and application to enzyme crosslinking," *Biotechniques*, vol. 37, no. 5, pp. 790–802, 2004.

- [30] D. Ucan, F. E. Kanik, Y. Karatas, and L. Toppare, "Synthesis and characterization of a novel polyphosphazene and its application to biosensor in combination with a conducting polymer," *Sensors Actuators, B Chem.*, vol. 201, pp. 545–554, 2014.
- [31] J. D. Newman and A. P. F. Turner, "Home blood glucose biosensors: A commercial perspective," *Biosens. Bioelectron.*, vol. 20, no. 12, pp. 2435–2453, 2005.
- [32] D. Fitzpatrick, "Glucose Biosensors," in *Implantable Electronic Medical Devices*, Elsevier, 2015, pp. 37–51.
- [33] C. Chen *et al.*, "Recent advances in electrochemical glucose biosensors: a review," *RSC Adv.*, vol. 3, no. 14, p. 4473, 2013.
- [34] A. L. Galant, R. C. Kaufman, and J. D. Wilson, "Glucose: Detection and analysis," *Food Chem.*, vol. 188, pp. 149–160, 2015.
- [35] J. Wang, "Electrochemical Glucose Biosensors," *Chem. Rev.*, vol. 108, pp. 814–825, 2008.
- [36] V. Leskovac, S. Trivić, G. Wohlfahrt, J. Kandrač, and D. Peričin, "Glucose oxidase from *Aspergillus niger*: The mechanism of action with molecular oxygen, quinones, and one-electron acceptors," *Int. J. Biochem. Cell Biol.*, vol. 37, no. 4, pp. 731–750, 2005.
- [37] E.-H. Yoo and S.-Y. Lee, "Glucose Biosensors: An Overview of Use in Clinical Practice," *Sensors*, vol. 10, no. 5, pp. 4558–4576, 2010.
- [38] H. Shirakawa, "The discovery of polyacetylene film - The dawning of an era of conducting polymers," *Curr. Appl. Phys.*, vol. 1, no. 4–5, pp. 281–286, 2001.
- [39] H. Shirakawa, J. Louis, and A. G. Macdiarmid, "Synthesis of Electrically Conducting Organic Polymers: Halogene Derivatives of Polyacetylene, (CH)<sub>x</sub>," *J. C. S. Chem. Comm.*, no. 578, pp. 578–580, 1977.
- [40] A. J. Heeger, "Semiconducting and Metallic Polymers: The Fourth Generation of Polymeric Materials (Nobel Lecture) Copyright(c) The Nobel Foundation 2001. We thank the Nobel Foundation, Stockholm, for permission to print this lecture.," *Angew. Chem. Int. Ed. Engl.*, vol. 40, no. 14, pp. 2591–2611, 2001.
- [41] a J. Heeger, "Nobel Lecture: Simuconducting and Metallic Polymers: The Fourth Generation of Polymeric Materials.," *Rev. Mod. Phys.*, vol. 73, no. 36, p. 681, 2001.
- [42] A. G. MacDiarmid, "'Synthetic Metals': A Novel Role for Organic Polymers," *Angew. Chem. Int. Ed. Engl.*, vol. 40, no. 14, pp. 2581–2590, 2001.
- [43] A. G. MacDiarmid, "'Synthetic metals': A novel role for organic polymers (Nobel lecture)," *Angew. Chemie - Int. Ed.*, vol. 40, no. 14, pp. 2581–2590, 2001.
- [44] J. L. Reddinger and J. R. Reynolds, "Molecular Engineering of nxonjugated

- Polymers,” in *Advances in Polymer Science*, 145th ed., Berlin, Heidelberg: Springer, 1999.
- [45] B. D. Malhotra, A. Chaubey, and S. P. Singh, “Prospects of conducting polymers in biosensors,” *Anal. Chim. Acta*, vol. 578, no. 1, pp. 59–74, 2006.
- [46] Y.-J. Cheng, S.-H. Yang, and C.-S. Hsu, “Synthesis of Conjugated Polymers for Organic Solar Cell Applications,” *Chem. Rev. (Washington, DC, U. S.)*, vol. 109, no. 11, pp. 5868–5923, 2009.
- [47] J. L. Bredas and G. B. Street, “Polarons , Bipolarons , and Solitons in Conducting Polymers,” *Acc. Chem. Res.*, vol. 18, pp. 309–315, 1985.
- [48] K. Arshak, V. Velusamy, O. Korostynska, K. Oliwa-stasiak, and C. Adley, “Conducting Polymers and Their Applications to Biosensors : Emphasizing on Foodborne Pathogen Detection Conducting Polymers and Their Applications to Biosensors : Emphasizing on Foodborne Pathogen Detection,” *IEEE Sens. J.*, vol. 9, no. 12, pp. 1942–1951, 2009.
- [49] M. Angelopoulos, “Conducting polymers in microelectronics Conjugated polymers in the nondoped and,” *IBM J. Res. Dev.*, vol. 45, no. 1, pp. 57–75, 2001.
- [50] G. G. Wallace, M. Smyth, and H. Zhao, “Conducting electroactive polymer-based biosensors,” *TrAC - Trends Anal. Chem.*, vol. 18, no. 4, pp. 245–251, 1999.
- [51] P. Chandrasekhar, *Conducting Polymers, Fundamentals and Applications: A Practical Approach*. New York: Springer Science & Business Media, 2013.
- [52] W. Schuhmann, “Conducting Polymer Based Amperometric Enzyme Electrodes,” *Microchim. Acta*, vol. 121, pp. 1–29, 1995.
- [53] A. P.M. and Z. O.Z., “Carbon Nanotubes,” in *Topics in Applied Physics*, 80th ed., D. M.S., D. G., and A. P., Eds. Berlin, Heidelberg: Springer, 2001.
- [54] W. Yang, K. R. Ratinac, S. R. Ringer, P. Thordarson, J. J. Gooding, and F. Braet, “Carbon nanomaterials in biosensors: Should you use nanotubes or graphene,” *Angew. Chemie - Int. Ed.*, vol. 49, no. 12, pp. 2114–2138, 2010.
- [55] S. Gupta, C. N. Murthy, and C. R. Prabha, “Recent advances in carbon nanotube based electrochemical biosensors,” *Int. J. Biol. Macromol.*, vol. 108, pp. 687–703, 2018.
- [56] J. Wang, “Carbon-nanotube based electrochemical biosensors: A review,” *Electroanalysis*, vol. 17, no. 1, pp. 7–14, 2005.
- [57] N. Yang, X. Chen, T. Ren, P. Zhang, and D. Yang, “Carbon nanotube based biosensors,” *Sensors Actuators, B Chem.*, vol. 207, no. PartA, pp. 690–715, 2015.
- [58] Y. Rio, M. S. Rodríguez-Morgade, and T. Torres, “Modulating the electronic properties of porphyrinoids: A voyage from the violet to the infrared regions of

- the electromagnetic spectrum,” *Org. Biomol. Chem.*, vol. 6, no. 11, pp. 1877–1894, 2008.
- [59] G. De La Torre, C. G. Claessens, and T. Torres, “Phthalocyanines: Old dyes, new materials. Putting color in nanotechnology,” *Chem. Commun.*, no. 20, pp. 2000–2015, 2007.
- [60] G. de la Torre, G. Bottari, U. Hahn, and T. Torres, *Functional Phthalocyanines: Synthesis, Nanostructuring, and Electro-Optical Applications*, 135th ed. Berlin, Heidelberg: Springer, 2010.
- [61] K. Sakamoto and E. Ohno-Okumura, “Syntheses and functional properties of phthalocyanines,” *Materials (Basel)*, vol. 2, no. 3, pp. 1127–1179, 2009.
- [62] A. Lütfti Uğur, A. Erdoğan, A. Koca, and U. Avciata, “Synthesis, spectroscopic, electrochemical and spectroelectrochemical properties of metal free, manganese, and cobalt phthalocyanines bearing peripherally octakis-[4-(thiophen-3-yl)-phenoxy] substituents,” *Polyhedron*, vol. 29, no. 18, pp. 3310–3317, 2010.
- [63] L. Cui, G. Lv, and X. He, “Enhanced oxygen reduction performance by novel pyridine substituent groups of iron (II) phthalocyanine with graphene composite,” *J. Power Sources*, vol. 282, pp. 9–18, 2015.
- [64] Y. Jiang *et al.*, “Enhanced catalytic performance of Pt-free iron phthalocyanine by graphene support for efficient oxygen reduction reaction,” *ACS Catal.*, vol. 3, no. 6, pp. 1263–1271, 2013.
- [65] D. Liu and Y. T. Long, “Superior Catalytic Activity of Electrochemically Reduced Graphene Oxide Supported Iron Phthalocyanines toward Oxygen Reduction Reaction,” *ACS Appl. Mater. Interfaces*, vol. 7, no. 43, pp. 24063–24068, 2015.
- [66] R. Devasenathipathy *et al.*, “A sensitive and selective enzyme-free amperometric glucose biosensor using a composite from multi-walled carbon nanotubes and cobalt phthalocyanine,” *RSC Adv.*, vol. 5, no. 34, pp. 26762–26768, 2015.
- [67] G. Bottari, O. Trukhina, M. Ince, and T. Torres, “Towards artificial photosynthesis: Supramolecular, donor-acceptor, porphyrin- and phthalocyanine/carbon nanostructure ensembles,” *Coord. Chem. Rev.*, vol. 256, no. 21–22, pp. 2453–2477, 2012.
- [68] E. Buhleier, W. Wehner, and F. Vögtle, “‘Cascade’- and ‘nonskid-chain-like’ syntheses of molecular cavity topologies,” *Synthesis (Stuttg.)*, pp. 155–158, 1978.
- [69] R. G. Denkewalter, J. Kolc, and W. J. Lukasavage, “Macromolecular highly branched homogeneous compound based on lysine units,” US Patent 4,289,872, 1981.
- [70] D. A. Tomalia *et al.*, “A New Class of Polymers: Starburst-Dendritic

- Macromolecules,” *Polym. J.*, vol. 17, no. 1, pp. 117–132, 1985.
- [71] G. R. Newkome, Z. Yao, G. R. Baker, and V. K. Gupta, “Micelles. Part 1. Cascade molecules: a new approach to micelles. A [27]-arborol,” *J. Org. Chem.*, vol. 50, no. 11, pp. 2003–2004, 1985.
- [72] C. C. Lee, J. A. MacKay, J. M. J. Fréchet, and F. C. Szoka, “Designing dendrimers for biological applications,” *Nat. Biotechnol.*, vol. 23, no. 12, pp. 1517–1526, 2005.
- [73] M. Fischer and F. Vögtle, “Dendrimers: From Design to Application—A Progress Report,” *Angew. Chemie Int. Ed.*, vol. 38, no. 7, pp. 884–905, 1999.
- [74] A. W. Bosman, H. M. Janssen, and E. W. Meijer, “About Dendrimers: Structure, Physical Properties, and Applications,” *Chem. Rev.*, vol. 99, no. 7, pp. 1665–1688, 1999.
- [75] H. C. Yoon and H. S. Kim, “Multilayered assembly of dendrimers with enzymes on gold: Thickness- controlled biosensing interface,” *Anal. Chem.*, vol. 72, no. 5, pp. 922–926, 2000.
- [76] J. Satija, V. V. R. Sai, and S. Mukherji, “Dendrimers in biosensors: Concept and applications,” *J. Mater. Chem.*, vol. 21, no. 38, pp. 14367–14386, 2011.
- [77] D. M. Kima, M. A. Rahmanb, M. H. Do, C. Ban, and Y. B. Shim, “An amperometric chloramphenicol immunosensor based on cadmium sulfide nanoparticles modified-dendrimer bonded conducting polymer,” *Biosens. Bioelectron.*, vol. 25, no. 7, pp. 1781–1788, 2010.
- [78] D. K. Smith, “Dendritic supermolecules - Towards controllable nanomaterials,” *Chem. Commun.*, no. 1, pp. 34–44, 2006.
- [79] B. Kavosi, A. Salimi, R. Hallaj, and K. Amani, “A highly sensitive prostate-specific antigen immunosensor based on gold nanoparticles/PAMAM dendrimer loaded on MWCNTS/chitosan/ionic liquid nanocomposite,” *Biosens. Bioelectron.*, vol. 52, pp. 20–28, 2014.
- [80] M. Pan, L. Kong, B. Liu, K. Qian, G. Fang, and S. Wang, “Production of multi-walled carbon nanotube/poly(aminoamide) dendrimer hybrid and its application to piezoelectric immunosensing for metolcarb,” *Sensors Actuators, B Chem.*, vol. 188, pp. 949–956, 2013.
- [81] L. Gorton, “Carbon paste electrodes modified with enzymes, tissues, and cells,” *Electroanalysis*, vol. 7, no. 1, pp. 23–45, 1995.
- [82] C. W. Pratt and K. Cornely, *Essential Biochemistry*, 3rd ed. John Wiley & Sons, Inc, 2014.
- [83] A. Cornish-Bowden, *Principles of Enzyme Kinetics*. London, England: Butterworth&Co, 1976.
- [84] K. Wang, J. J. Xu, and H. Y. Chen, “A novel glucose biosensor based on the nanoscaled cobalt phthalocyanine-glucose oxidase biocomposite,” *Biosens.*

*Bioelectron.*, vol. 20, no. 7, pp. 1388–1396, 2005.

- [85] K. I. Ozoemena and T. Nyokong, “Novel amperometric glucose biosensor based on an ether-linked cobalt(II) phthalocyanine-cobalt(II) tetraphenylporphyrin pentamer as a redox mediator,” *Electrochim. Acta*, vol. 51, no. 24, pp. 5131–5136, 2006.
- [86] Y. Qin, Y. Kong, Y. Xu, F. Chu, Y. Tao, and S. Li, “In situ synthesis of highly loaded and ultrafine Pd nanoparticles-decorated graphene oxide for glucose biosensor application,” *J. Mater. Chem.*, vol. 22, no. 47, pp. 24821–24826, 2012.
- [87] X. Pang, P. Imin, I. Zhitomirsky, and A. Adronov, “Amperometric detection of glucose using a conjugated polyelectrolyte complex with single-walled carbon nanotubes,” *Macromolecules*, vol. 43, no. 24, pp. 10376–10381, 2010.
- [88] Y. Q. Zhang *et al.*, “A novel glucose biosensor based on the immobilization of glucose oxidase on layer-by-layer assembly film of copper phthalocyanine functionalized graphene,” *Electrochim. Acta*, vol. 104, pp. 178–184, 2013.
- [89] H. Zhao and H. Ju, “Multilayer membranes for glucose biosensing via layer-by-layer assembly of multiwall carbon nanotubes and glucose oxidase,” *Anal. Biochem.*, vol. 350, no. 1, pp. 138–144, 2006.
- [90] Y. Chen, Y. Li, D. Sun, D. Tian, J. Zhang, and J. J. Zhu, “Fabrication of gold nanoparticles on bilayer graphene for glucose electrochemical biosensing,” *J. Mater. Chem.*, vol. 21, no. 21, pp. 7604–7611, 2011.
- [91] M. Holzinger, L. Bouffier, R. Villalonga, and S. Cosnier, “Adamantane/ $\beta$ -cyclodextrin affinity biosensors based on single-walled carbon nanotubes,” *Biosens. Bioelectron.*, vol. 24, no. 5, pp. 1128–1134, 2009.
- [92] S. Zhang, N. Wang, Y. Niu, and C. Sun, “Immobilization of glucose oxidase on gold nanoparticles modified Au electrode for the construction of biosensor,” *Sensors Actuators, B Chem.*, vol. 109, no. 2, pp. 367–374, 2005.
- [93] S. Demirci *et al.*, “Functionalization of poly-SNS-anchored carboxylic acid with Lys and PAMAM: Surface modifications for biomolecule immobilization/stabilization and bio-sensing applications,” *Analyst*, vol. 137, no. 18, pp. 4254–4261, 2012.
- [94] E. Matsumoto, T. Fukuda, and Y. Miura, “Bioinert surface to protein adsorption with higher generation of dendrimer SAMs,” *Colloids Surfaces B Biointerfaces*, vol. 84, no. 1, pp. 280–284, 2011.
- [95] W. Zhang *et al.*, “Multifunctional glucose biosensors from Fe<sub>3</sub>O<sub>4</sub> nanoparticles modified chitosan/graphene nanocomposites,” *Sci. Rep.*, vol. 5, no. 1, p. 11129, 2015.
- [96] J. Singh *et al.*, “Preparation of sulfonated poly(ether-ether-ketone) functionalized ternary graphene/AuNPs/chitosan nanocomposite for efficient glucose biosensor,” *Process Biochem.*, vol. 48, no. 11, pp. 1724–1735, 2013.

- [97] E. Araque, C. B. Arenas, M. Gamella, J. Reviejo, R. Villalonga, and J. M. Pingarrón, "Graphene-polyamidoamine dendrimer-Pt nanoparticles hybrid nanomaterial for the preparation of mediatorless enzyme biosensor," *J. Electroanal. Chem.*, vol. 717–718, pp. 96–102, 2014.
- [98] E. G. R. Fernandes and A. A. A. De Queiroz, "A bioconjugated polyglycerol dendrimer with glucose sensing properties," *J. Mater. Sci. Mater. Med.*, vol. 20, no. 2, pp. 473–479, 2009.
- [99] Y. Liu, M. Wang, F. Zhao, Z. Xu, and S. Dong, "The direct electron transfer of glucose oxidase and glucose biosensor based on carbon nanotubes/chitosan matrix," *Biosens. Bioelectron.*, vol. 21, no. 6, pp. 984–988, 2005.
- [100] S. Palanisamy, S. Cheemalapati, and S. M. Chen, "Amperometric glucose biosensor based on glucose oxidase dispersed in multiwalled carbon nanotubes/graphene oxide hybrid biocomposite," *Mater. Sci. Eng. C*, vol. 34, no. 1, pp. 207–213, 2014.
- [101] M. Şenel, C. Nergiz, and E. Çevik, "Novel reagentless glucose biosensor based on ferrocene cored asymmetric PAMAM dendrimers," *Sensors Actuators, B Chem.*, vol. 176, pp. 299–306, 2013.
- [102] M. Snejdarkova, L. Svobodova, V. Gajdos, and T. Hianik, "Glucose biosensors based on dendrimer monolayers," *J. Mater. Sci. Mater. Med.*, vol. 12, no. 10–12, pp. 1079–1082, 2001.
- [103] C. X. Guo, Z. M. Sheng, Y. Q. Shen, Z. L. Dong, and C. M. Li, "Thin-walled graphitic nanocages as a unique platform for amperometric glucose biosensor," *ACS Appl. Mater. Interfaces*, vol. 2, no. 9, pp. 2481–2484, 2010.
- [104] E. Buber, A. Yuzer, S. Soylemez, M. Kesik, M. Ince, and L. Toppare, "Construction and amperometric biosensing performance of a novel platform containing carbon nanotubes-zinc phthalocyanine and a conducting polymer," *Int. J. Biol. Macromol.*, vol. 96, pp. 61–69, 2017.
- [105] E. Buber, M. Kesik, S. Soylemez, and L. Toppare, "A bio-sensing platform utilizing a conjugated polymer, carbon nanotubes and PAMAM combination," *J. Electroanal. Chem.*, vol. 799, no. May, pp. 370–376, 2017.